Published November 24, 2008

Transfer of autoimmune exocrinopathy in *RbAp48*-Tg mice

Because thymic T cell abnormality could not be observed in *RbAp48*-Tg mice, it is speculated that there may be dysregulation of peripheral tolerance. To know the homeostatic expansion of peripheral T cells from *RbAp48*-Tg mice, we adoptively transferred CFSE-labeled $CD4^+$ T cells from *RbAp48*-Tg mice into irradiated syngeneic C57BL/6.Ly5.1 mice and analyzed them 7 d later. As a result, we observed more substantial cell division of the donor CFSE-labeled cLN $CD4^+$ T cells from *RbAp48*-Tg mice than that from WT mice (Fig. 7 A), indicating that T cells undergoing homeostatic proliferation may provide a basis for autoimmunity (40, 41). This suggests that elicitation of $CD4^+$ T cell–mediated autoreactivity against autoantigen could be the primary pathogenic process that leads to substantial homeostatic expansion. Furthermore, we succeeded in adoptive transfer of autoimmune lesions in the exocrine glands into $Rag2^{-/-}$ mice using cervical lymph node cells, but not spleen cells, from *RbAp48*-Tg mice (Fig. 7, B and C). Interestingly, these transferred lesions were extremely enhanced in estrogen-deficient $Rag2^{-/-}$ mice treated with ovariectomy (Ovx) compared with the lesions in Sham $Rag2^{-/-}$ mice (Fig. 7, D and F), suggesting that estrogen deficiency accelerates autoimmune exocrinopathy, as previously reported (21, 22). When we examined the adoptive

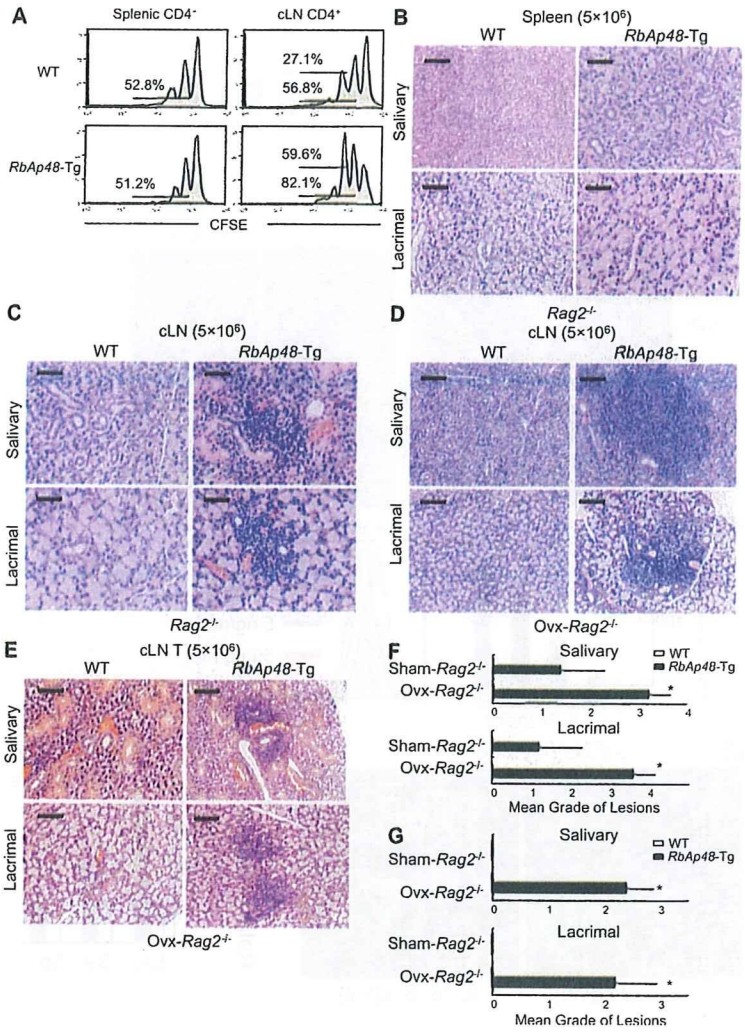

Figure 7. Transfer of autoimmune lesions from *RbAp48*-Tg mice into $Rag2^{-/-}$ mice. (A) Homeostatic proliferation of splenic and cLN T cells from WT and *RbAp48*-Tg mice at 28 wk of age was analyzed at 7 d after transfer into irradiated C57BL/6 mice. Results are representative of four to five mice in two independent experiments. Percentages of divided cells from the second or third division are indicated. (B and C) Spleen cells (5×10^6) or cLN cells (5×10^6) from WT and *RbAp48*-Tg mice at 30 wk of age were transferred into $Rag2^{-/-}$ mice. At 6 wk after the transfer, the pathology of salivary and lacrimal glands was analyzed. Images are representative of four to five mice. (D) cLN cells from WT and *RbAp48*-Tg mice were transferred into ovariectomized (Ovx) $Rag2^{-/-}$ mice. (E) T cells of cLNs from WT and *RbAp48*-Tg mice were transferred into ovariectomized (Ovx) $Rag2^{-/-}$ mice. Images of salivary and lacrimal gland tissues were representative of four to five mice. (F) Severity of inflammatory lesions of salivary and lacrimal glands from sham-operated (Sham) and Ovx-$Rag2^{-/-}$ hosts by transfer of cLN cells were shown as mean grade of lesions. (G) Severity of inflammatory lesions of salivary and lacrimal glands from sham-operated (Sham) and Ovx-$Rag2^{-/-}$ hosts by T cell transfer were shown as mean grade of lesions. Data are shown as means ± SE of four to five mice. *, $P < 0.05$, Sham versus Ovx. Bars: (B–E) 100 µm.

Published November 24, 2008

transfer using T cells isolated from cervical lymph nodes and spleen of *RbAp48*-Tg mice, no inflammatory lesions had developed in *Rag2*$^{-/-}$ mice (Table I). These data suggest that APCs besides T cells might be required for successful transfer of autoimmune exocrinopathy in *RbAp48*-Tg mice. Finally, to confirm that MHC class II expression on activated salivary or lacrimal gland cells of *RbAp48*-Tg mice can drive priming of purified T cells of cLNs from *RbAp48*-Tg mice to induce autoimmune lesions, the T cells of cLNs from *RbAp48*-Tg mice were transferred into Ovx-*Rag2*$^{-/-}$ mice. The autoimmune lesions of salivary and lacrimal glands from the recipient Ovx-*Rag2*$^{-/-}$ mice transferred with T cells of cLNs from *RbAp48*-Tg mice were observed, whereas no lesions were found in any organs of the recipient Ovx-*Rag2*$^{-/-}$ mice transferred with T cells of cLNs from WT mice (Fig. 7, E and G). These results demonstrate that the epithelial cells stimulated through increased RbAp48 because of estrogen deficiency could interact with T cells to induce autoimmunity via loss of local tolerance.

Table I. Induction of autoimmune lesions

Donor cells	Mice	Incidence
Spleen cells (5 × 10^6)	WT	0/4
	RbAp48-Tg	0/4
cLN cells (5 × 10^6)	WT	0/5
	RbAp48-Tg	4/5
cLN T cells (5 × 10^6)	WT	0/4
	RbAp48-Tg	0/5
cLN B cells (5 × 10^6)	WT	0/4
	RbAp48-Tg	0/4

Whole spleen, cLN cells, cLN T cells, or cLN B cells were transferred intravenously into *Rag2*$^{-/-}$ mice. The host mice were killed 6 wk after transfer. Inflammatory lesions of salivary or lacrimal glands were evaluated by pathological analysis.

IFN-γ and IL-18 expressions in human SS patients

Although it has been reported that immune cells express some cytokines, it is unclear whether IFN-γ or IL-18 together with RbAp48 in the epithelial cells of salivary glands from human SS patients are expressed. To confirm our hypothesis that autoimmunity is induced by a breakdown of local tolerance in salivary gland cells with up-regulated RbAp48 because of estrogen deficiency such as menopause, IFN-γ, IL-18, and RbAp48 expressions were detected by confocal microscopic analysis using human biopsy samples from SS patients and controls. Among 10 SS patients, RbAp48$^+$ and IFN-γ$^+$ epithelial cells were observed in three samples and RbAp48$^+$ and IL-18$^+$ epithelial cells were observed in four samples. A representative image of SS patients and controls is shown in Fig. 8. Although faint expressions of RbAp48 in the nucleus of salivary epithelial cells were detected in control samples, IL-18 or IFN-γ together with a prominent expression of RbAp48 was not observed (Fig. 8). Isotype-matched controls of staining for the mAbs were shown in Fig. S10 (available at http://www.jem.org/cgi/content/full/jem.20080174/DC1).

DISCUSSION

Although MHC class II molecules have been expressed aberrantly on epithelial cells in association with autoimmunity, it remains debatable whether class II molecules are the initiating event or the consequence of the autoimmune attack. For example, certain alleles of class II (mouse I-A^{g7}) might be particularly good at presenting glutamic acid decarboxylase–65 or insulin peptides to T cells in nonobese diabetic (NOD) mice, thus contributing to recognition and ultimate destruction of pancreatic β cells (10, 11). Some investigators have proposed that I-A^{g7}, because of its poor peptide-binding properties, enhances autoimmunity in NOD mice in a global fashion (42). In this case, the β cell specificity of autoimmunity in this strain and the switch to autoimmune thyroiditis when a class II molecule without these properties is exchanged for I-A^{g7} must be controlled by other genetic loci in NOD mice (43). It is possible that the most straightforward explanation for the effects of I-A^{g7} is that it predisposes to

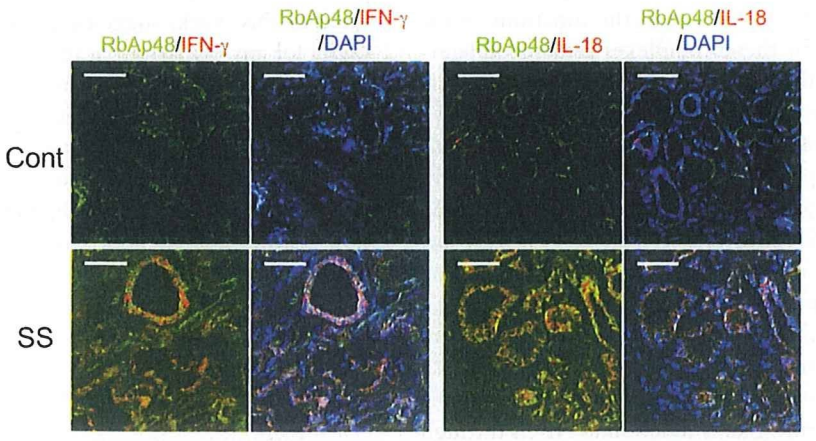

Figure 8. IFN-γ and IL-18 expressions together with RbAp48 in salivary glands from SS patients. The frozen sections of salivary glands from SS patients and controls were stained with IFN-γ or IL-18 (Alexa Fluor 568; red) and RbAp48 (Alexa Fluor 488; green) mAbs. The nuclei were stained with DAPI. The representative images in controls and SS patients were shown in three independent experiments.

Published November 24, 2008

islet-specific autoimmunity and not system-wide reactivity. Another piece of evidence that the role of MHC class II is antigen-specific is that the class II alleles predisposing toward autoimmunity vary in one human disease to another, indicating that class II alleles act in autoimmunity via specific antigens rather than comprehensively.

We demonstrated in this study that autoimmune exocrinopathy resembling SS developed in almost all *RbAp48*-Tg mice, and that a high titer of serum autoantibodies against SS-A (Ro), SS-B (La), and 120-kD α-fodrin was detected in these Tg mice. We frequently found MHC class II molecule expression on the exocrine gland cells with autoimmune lesions in *RbAp48*-Tg mice. When we examined whether salivary epithelial cells could act on antigen presentation, we found a large proportion of MHC class II^+, $CD86^+$, $CD80^+$, and ICAM-1^+ cells primarily observed on cultured MSG cells from Tg mice. Moreover, CFSE-labeled purified $CD4^+$ (10^5) T cells from *RbAp48*-Tg mice were capable of responding to MSG cells from *RbAp48*-Tg mice, whereas anti–MHC class II antibody inhibited these responses. Although it has not been determined whether MHC class II–expressing epithelial cells can function as APCs, those data strongly suggest that the epithelial cells may function as APCs during development of autoimmune exocrinopathy. In *RbAp48*-Tg mice, a surprisingly prominent expression of epithelial IFN-γ was detected beside sporadically positive infiltrating cells. These findings were observed mainly in the MHC class II^+ ductal epithelium adjacent to lymphoid infiltrates. Epithelial IFN-γ expression in the exocrine glands of *RbAp48*-Tg mice was up-regulated during the course of autoimmune exocrinopathy. A previously unknown, multifaceted role of IFN-γ as regulator of the local immune system, which is termed here local tolerance, is disclosed. As to the mechanism of CIITA induction in *RbAp48*-Tg mice, our findings demonstrate the essential role of RbAp48-driven stimulation of IFN-γ production and signaling leading to up-regulation of IRF-1 and CIITA. RbAp48, initially identified as retinoblastoma-binding proteins (44), was characterized as a component of distinct nucleosome-modifying complexes, including the nuclear histone deacetylases (45, 46). Although the functions of the RbAp48-like proteins in these complexes remain undetermined, it was reported that E2F-1 and RbAp48 are physically associated in the presence of Rb and histone deacetylase (47), suggesting that RbAp48 could be involved in transcriptional repression of E2F-responsive genes. Several reports have demonstrated that estrogen may play an inhibitory role on apoptosis in endothelial cells, breast cancer cells, cardiac myocytes, prostate cells, and neuronal cells (48–51). It has been shown that the transcription factor IRF-1 mRNA expression is induced by ICI 182,780 as an antiestrogenic reagent and repressed by estrogens in antiestrogen-sensitive cells (52). We demonstrated the first evidence that IFN-γ–producing epithelial cells in the exocrine glands function as APCs through the IRF-1–CIITA pathway, resulting in the development of autoimmune exocrinopathy via loss of local tolerance. SS is known to have the most female predominance of >95% among all the autoimmune patients (15, 16). One of the key questions in respect to the pathophysiology of autoimmune diseases is how autoreactivity to particular autoantigens is initiated and maintained under an estrogen-deficient state. Although an important role for T cells in the development of autoimmune disease has been argued (53, 54), it is not known if disease is initiated by a retrained inflammatory reaction to autoantigen. We clarified that epithelial IFN-γ production is crucial for the initiation of autoimmune reactions between epithelial cells and autoreactive T cells with homeostatic expansion. Our previous study suggests that antiestrogenic actions have a potent effect on the proteolysis of α-fodrin autoantigen in the salivary gland through up-regulation of caspase 1 activity (22). These results strongly suggest that RbAp48-mediated activation of caspase 1 leads to the cleavage and activation of IL-18, which may act directly on IFN-γ production and on effector $CD4^+$ T cells by inducing migration and proliferation. Thus, aberrant expression of MHC class II in the exocrine glands facilitates loss of local tolerance before the development of autoimmune lesions, which is very similar to SS.

Evidence has been mounting that estrogen deficiency such as menopause is a proinflammatory state, which promotes osteoporosis and atherosclerosis, as well as autoimmunity (55, 56). In vivo and in vitro experiments here, including the induction of autoimmune lesions by T cell transfer from *RbAp48*-Tg mice into Ovx-*Rag2*$^{-/-}$ mice and in vitro antigen presentation of the Tg MSG cells to $CD4^+$ T cells, strongly suggests that estrogen deficiency stimulates salivary epithelial cells that are activated via the up-regulation of RbAp48 to present any endogenous autoantigen to $CD4^+$ T cells for the onset of autoimmune lesion in the salivary glands resembling human SS. Our data finds that transfer of cLN T cells from *RbAp48*-Tg mice into Ovx-*Rag2*$^{-/-}$ mice leads to autoimmune lesions, consistent with the conclusion that estrogen deficiency leads to the ability of salivary gland epithelial cells to express MHC class II and present any self-antigens. Most importantly, the salivary gland cells from human SS patients express RbAp48 together with IFN-γ or IL-18, as well as the findings of *RbAp48*-Tg mice in this work, suggesting that the molecules would be useful for any clinical application.

Collectively, our results demonstrate a direct molecular mechanism by which estrogen deficiency induces tissue-specific overexpression of RbAp48 (23), subsequently developing $CD4^+$ T cell–mediated autoimmunity through epithelial IFN-γ production. Thus, reducing the RbAp48 overexpression is a possible effective therapy in gender-based autoimmune exocrinopathy.

MATERIALS AND METHODS

Mice and histology. *RbAp48*-Tg mice have been previously described (23), and the RbAp48 gene is regulated by lacrimal and salivary gland-specific promoter (57). *Rag2*$^{-/-}$ mice were obtained from Taconic. All mice were reared in our specific pathogen–free mouse colony, and given food and water ad libitum. The experiments were approved by an animal ethics board of Tokushima University. All organs were removed from the mice, fixed with 4% phosphate-buffered formaldehyde (pH 7.2), and prepared for

histological examination. Formalin-fixed tissue sections were subjected to hematoxylin and eosin (H&E) staining, and three pathologists independently evaluated the histology without being informed of the condition of each individual mouse. Histological grading of the inflammatory lesions was done according to the method proposed by White and Casarett (58), as follows: 1 = 1–5 foci composed of >20 mononuclear cells per focus, 2 = >5 such foci, but without significant parenchymal destruction, 3 = degeneration of parenchymal tissue, and 4 = extensive infiltration of the glands with mononuclear cells and extensive parenchymal destruction. Histological evaluation of the salivary and lacrimal glands was performed in a blind manner, and a tissue section from each salivary and lacrimal gland was examined.

Measurement of fluid secretion. Analysis of the tear and saliva volume of WT and *RbAp48*-Tg mice was performed according to a previously described method (59).

Flow cytometric analysis. Lymphocytes in spleen, cLN, thymus, and MSG epithelial cells without immune cells (>95% of cells were keratin$^+$) were prepared. Surface markers were identified by mAbs with an EPICS flow cytometer (Beckman Coulter). Rat mAbs to FITC-, PE-, or PE-Cy5-conjugated anti-B220, CD4, MHC class II, CD86, CD80, ICAM1, and CD5 mAbs (eBioscience) were used. Appropriate isotype-matched controls were used, respectively. For detection of T cell activation markers, FITC-conjugated anti-CD25, CD44, CD62L, CD45RB, and CD69 mAbs (eBioscience) were used. Intracellular Foxp3 expression with an Intracellular Foxp3 Detection kit (eBioscience) was performed according to the manufacturer's instructions. Detections of intracellular IFN-γ or IL-18 were also performed by the same procedure. The data were analyzed with FlowJo FACS Analysis software (Tree Star, Inc.).

ELISA. The amount of mouse IL-2, IFN-γ, IL-4, and IL-10 in culture supernatants from CD4$^+$ T cells stimulated with anti-TCR mAb (~0–1 μg/ml) and anti-CD28 mAb (20 μg/ml; eBioscience), anti-SSA, anti-SSB, and anti–α-fodrin autoantibodies of sera from WT and *RbAp48*-Tg mice and human IL-18 and IFN-γ from cultured HSG and MCF-7 cells were analyzed by ELISA. In brief, plates were coated with a capture antibody or recombinant proteins (SSA, SSB, and α-fodrin), and washed with PBS/0.1% Tween 20. The plates were incubated with diluted culture supernatants or sera. After washing with PBS/0.1% Tween 20 and incubation of biotin-conjugated antibodies for cytokine detection, a horseradish peroxidase–conjugated detection antibody for autoantibody detection was added. After incubation with streptavidin-horseradish peroxidase for cytokine detection, plates were again washed with PBS/0.1% Tween 20 and o-phenylendiamine (Sigma-Aldrich) buffer added. Plates were then analyzed with a microplate reader reading at 490 nm.

Confocal microscopic analysis. Confocal microscopic analysis using anti-Thy1.2, B220, CD4, CD8, MHC class II, IFN-γ, CD4 (eBioscience), keratin (LSL CO., LTD), and IL-18 (MBL) antibodies was performed on the frozen sections of salivary glands from WT and *RbAp48*-Tg mice, and on the cultured cells using Confocal Laser Microscan (LSM 5 PASCAL; Carl Zeiss, Inc.). As the second antibodies, Alexa Fluor 488 anti–mouse IgG (H+L), Alexa Fluor 568 goat anti–rabbit IgG (H+L), Alexa Fluor 488 donkey anti–rat IgG (H+L), Alexa Fluor 488 chicken anti–goat IgG (H+L), and Alexa Fluor 568 rabbit anti–goat IgG (H+L; Invitrogen) were used. The nuclear DNA was stained with DAPI (Invitrogen).

Cell culture. For the co-culture of MSG with CD4$^+$ T cells, MSG cells were prepared by digestion of collagenase and hyaluronidase, and CD11c$^+$, CD11b$^+$, B220$^+$, NK1.1$^+$, and Thy1.2$^+$ cells were removed by the mAbs and magnetic bead–conjugated anti–rat IgG (Invitrogen). CD4$^+$ T cells from cLNs were purified by mAbs (anti-MHC class II, CD8, CD11b, CD11c, B220, and NK1.1) and magnetic bead–conjugated anti–rat IgG. CFSE-labeled CD4$^+$ T cells were co-cultured with MSG cells for 72 h. Cell division of CD4$^+$ T cells was analyzed by dilution of CFSE through flow cytometry.

As for the co-culture with DCs or MSG cells, DCs from *RbAp48*-Tg or WT mice were enriched using DC collection kit (Invitrogen). After DCs or MSG cells were irradiated (9 Gy), purified CD4$^+$ T cells of cLNs from RbAp48-Tg mice were co-cultured with the DCs or MSG cells for 72 h. The T cells were then pulsed with 0.5 μCi [^{3}H]thymidine per well for the last 12 h of the culture. [^{3}H]thymidine incorporation was evaluated using an automated β liquid scintillation counter. HSG and MCF-7 cells were cultured in DME containing 10% FBS at 37°C. Tam (Wako Pure Chemical), 17β-estradiol (Wako), 10 μM caspase 1 inhibitor (Sigma-Aldrich), and recombinant human IFN-γ (R&D Systems) were used for cell cultures. RbAp48 gene inserted into pCMV (2N3T) construct (a gift from D. Trouche, Centre National de la Recherche Scientifique, University of Tolouse, Tolouse, France) (47) was transfected into the cells using FuGENE6 Transfection Reagent (Roche). Small interfering RNA (siRNA) corresponding to coding sequence +136 to +156 of RbAp48 gene was synthesized by Hokkaido System Science: CGAGGAAUACAAAAUAUGGTT (sense), CCAUAUUUUGUAUUCCUCGTT (antisense). When the siRNA was transfected into HSG cells together with GFP plasmid, 73.4% of cells were found to be GFP$^+$ HSG cells by flow cytometric analysis. Furthermore, the relative protein expression of RbAp48 to β-actin was reduced to ~80% by the siRNA.

Real-time quantitative RT-PCR. Total RNA was extracted from cultured HSG and MCF-7 cells using ISOGEN (Wako Pure Chemical), and reverse transcribed. Transcript levels of IRF-1, CIITA, and β-actin were performed using PTC-200 DNA Engine Cycler (Bio-Rad Laboratories) with SYBR Premix Ex Taq (Takara). Primer sequences were as follows: IRF-1, forward 5′-ACCCTGGCTAGAGATGCAGA-3′ and reverse 5′-CCTTTTCCCCTGCTTTGTATCG-3′; CIITA, forward 5′-CAGGCAGCAGAGGAGAAGTTCACCATC-3′ and reverse 5′-CCGTGAGGATCCGCACCAGTTTGGGG-3′; β-actin, forward 5′-AAATCTGGCACCACACCTTC-3′ and reverse 5′-GAGGCGTACAGGGATAGCA-3′.

Caspase activity. Caspase activities were assayed using Caspase-Family Colorimetric Substrate Set (BioVision, Inc.). In brief, 100 μg cytoplasmic lysates from lacrimal glands, salivary glands, and spleen of WT and *RbAp48*-Tg mice were incubated with 200 μM Ac-YVAD-pNA (Caspase 1 substrate), at 37°C for 1 h. The absorbance of samples was read at 405 nm in a microplate reader.

Promoter assay. For the measurement of the transcriptional activity of IRF-1, IRF-1 luciferase reporter vector (IRF-1/Luc) was purchased from Panomics. HSG cells plated in a 48-well plate were transiently transfected with 0.1 μg of IRF-1/Luc and 0.1 μg of pCMV-*RbAp48* or mock plasmid and 0.05 μg of phRL-TK (Promega Corp.) as an internal control using the FuGENE6. The cells were incubated overnight and subsequently treated with IFN-γ. After 10 h, the cells were harvested and subjected to a luciferase assay by using a dual-luciferase reporter assay system (Promega Corp.) as per the manufacturer's instructions. Relative luciferase activity was expressed as the fold- increase relative to the activity of untreated controls after normalization to the relative background of Renilla luciferase activity.

Cell transfer. CFSE-labeled splenic and cLN T cells (5 × 10^6) from WT and *RbAp48*-Tg mice were intravenously transferred into irradiated (700 cGy) C57BL/6.Ly5.1 mice. On the seventh day after the transfer, spleen cells were analyzed to measure homeostatic proliferation via CFSE dilution by flow cytometry. For induction of autoimmune lesions, total cells, T cells, or B cells from spleen cells (5 × 10^6) or cLN cells (5 × 10^6) from WT and *RbAp48*-Tg mice were intravenously transferred into *Rag2*$^{-/-}$ mice. At 6 wk after the transfer, the pathology of all the organs, including salivary and lacrimal glands, was analyzed. In addition, *Rag2*$^{-/-}$ hosts were ovariectomized (Ovx) or sham operated (Sham). Adoptive cell transfer was performed on the next day after Ovx or Sham.

In situ hybridization. Mice were perfused transcardially with saline (0.9%) followed by 4% PFA. The salivary glands were collected and fixed in 4% PFA at 4°C for 3 h. 6 μm paraffin-embedded sections were prepared for ISH.

The RNA probe (587 bp) of mouse IFN-γ was produced by RT-PCR using primers (T3, AATTAACCCTCACTAAAGGGACTGGCAAAAGG-ATGGTGAC; T7, TAATACGACTCACTATAGGGAGATACAACCC-CGCAATCAC). Digoxigenin (DIG)-labeled antisense and sense control riboprobes were generated using DIG RNA labeling mix (Roche). The sections were pretreated with 10 μg/ml proteinase K for 10 min at room temperature and then hybridized with 1 μg/ml DIG-labeled probes at 45°C for 16 h. DIG was immunodetected with alkaliphosphatase-conjugated anti-DIG antibody. For positive controls, sections of spleen from lipopolysaccaride-injected mice were used. The probe was confirmed with the positive control sections, as shown in Fig. S6 B.

Human samples. Immunostaining for RbAp48 and IL-18 or IFN-γ were performed using lip biopsy samples from human SS patients and controls. All samples were obtained from the Tokushima University Hospital, Tokushima, Japan. This study was approved by certification of the ethics board of Tokushima University Hospital. All subjects signed a written informed consent before enrollment. All patients with SS were female, had documented xerostomia and keratoconjunctivitis sicca, and fulfilled the criteria of the Ministry of Health, Labor, and Welfare of Japan for the diagnosis of SS. All patients with SS had focus scores of greater than two in their lip biopsy and all tested positive for autoantibodies against Ro. Analysis was performed under the certification of the ethics board of Tokushima University Hospital. Frozen sections were stained with anti–human RbAp48 mAb (BD) and Alexa Fluor 488 donkey anti–mouse IgG (H+L; Invitrogen) and Biotin-conjugated anti-human IL-18 (MBL) or IFN-γ (eBioscience) mAbs and Alexa Fluor 568-conjugated streptavidin and analyzed by confocal microscopy. The nuclear DNA was DAPI.

Statistics. Student's *t* test was used for statistical analyses.

Online supplemental material. Fig. S1 shows T cell phenotypes of thymus from *RbAp48*-Tg and WT mice. Fig. S2 shows T reg cells of thymus, spleen, and cLN from *RbAp48*-Tg and WT mice. Fig. S3 shows B1 cells in salivary glands and marginal B cells of spleen and cLN from *RbAp48*-Tg and WT mice. Fig. S4 shows the purified MSG cells, and images of control staining for the expressions of MHC class II, CD86, CD80, ICAM-1, IFN-γ, and IL18. Fig. S5 shows IRF-1 and CIITA mRNA of MCF-7 cells stimulated with Tam or transfected with pCMV-*RbAp48*. Fig. S6 shows IFN-γ concentration of tissue homogenates of lacrimal, salivary, and spleen from *RbAp48*-Tg and WT mice, and control sections for in situ hybridization of IFN-γ mRNA. Fig. S7 shows BAFF expression of salivary glands and spleen from *RbAp48*-Tg and WT mice. Fig. S8 shows the time courses of IL-18, IFN-γ, and HLA-DR expressions of HSG cells stimulated Tam or transfected with pCMV-*RbAp48*. Fig. S9 shows IFN-γ secretion from MCF-7 in response to IL-18. Fig. S10 shows control staining for RbAp48 expression together with IFN-γ or IL-18 in salivary glands from human SS patients and controls. The online supplemental material is available at http://www.jem.org/cgi/content/full/jem.20080174/DC1.

The authors thank Ai Nagaoka and Noriko Kino for their technical assistance; Kumio J. Tanaka, Mizue Yamanaka, and Shino Niki of OurGenic Co., Ltd. for analysis by in situ hybridization; and Prof. Noriaki Takeda for analysis of samples of human SS patients.

This work was supported in part by a Grant-in-Aid for Scientific Research (nos. 17109016, and 17689049) from the Ministry of Education, Science, Sport, and Culture of Japan, and from the Uehara Memorial Foundation.

The authors have no conflicting financial interests.

Submitted: 25 January 2008
Accepted: 15 October 2008

REFERENCES

1. Richardson, B. 2007. Primer: epigenetics of autoimmunity. *Nat. Clin. Pract. Rheumatol.* 3:521–527.
2. Schoenborn, J.R., and C.B. Wilson. 2007. Regulation of interferon-g during innate and adaptive immune responses. *Adv. Immunol.* 96:41–101.
3. Mathews, M.B., and R.M. Bernstein. 1983. Myositis autoantibody inhibits histidyl-tRNA synthetase: a model for autoimmunity. *Nature.* 304:177–179.
4. Matsumoto, I., A. Staub, C. Benoist, and D. Mathis. 1999. Arthritis provoked by linked T and B cell recognition of a glycolytic enzyme. *Science.* 286:1732–1735.
5. Streilein, J.W., G.A. Wilbanks, and S.W. Cousins. 1992. Immunoregulatory mechanisms of the eye. *J. Neuroimmunol.* 39:185–200.
6. Griffith, T.S., T. Brunner, S.M. Fletcher, D.R. Green, and T.A. Ferguson. 1995. Fas ligand-induced apoptosis as a mechanism of immune privilege. *Science.* 270:1189–1192.
7. Steinman, L. 1996. Multiple sclerosis. A coordinated immunological attack against myelin in the central nervous system. *Cell.* 85:299–302.
8. Hutchings, P., L. O'Reilly, N.M. Parish, H. Waldmann, and A. Cooke. 1992. The use of a non-depleting anti-CD4 monoclonal antibody to re-establish tolerance to cells in NOD mice. *Eur. J. Immunol.* 22:1913–1918.
9. Haskins, K., and M. McDuffie. 1990. Acceleration of diabetes in young NOD mice with a $CD4^+$ islet-specific T cell clone. *Science.* 249:1433–1436.
10. Nepom, G.T., and W.W. Kwok. 1998. Molecular basis for HLA-DQ associations with IDDM. *Diabetes.* 47:1177–1184.
11. Stratmann, T., V. Apostolopoulos, V. Mallet-Designe, A.L. Corper, C.A. Scott, I.A. Wilson, A.S. Kang, and L. Teyton. 2000. The $I\text{-}A^{g7}$ MHC class II molecule linked to murine diabetes is a promiscuous peptide binder. *J. Immunol.* 165:3214–3225.
12. Londei, M., J.R. Lamb, G.F. Bottazzo, and M. Feldmann. 1984. Epithelial cell expressing aberrant MHC class II determinants can present antigen to cloned human T cells. *Nature.* 312:639–641.
13. He, X.L., C. Radu, J. Sidney, A. Sette, E.S. Ward, and K.C. Garcia. 2002. Structural snapshot of aberrant antigen presentation linked to autoimmunity: the immunodominant epitope of MBP complexed with I-Au. *Immunity.* 17:83–94.
14. Dallman, M.J., and D.W. Mason. 1983. Induction of Ia antigens on murine epidermal cells during the rejection of skin allografts. *Transplantation.* 36:222–224.
15. Whitacre, C.C., S.C. Reingold, and P.A. O'Looney. 1999. A gender gap in autoimmunity. *Science.* 283:1277–1278.
16. Whitacre, C.C. 2001. Sex differences in autoimmune disease. *Nat. Immunol.* 2:777–780.
17. Apostolou, I., Z. Hao, K. Rajewsky, and H. von Boehmer. 2003. Effective destruction of Fas-deficient insulin-producing β cells in type 1 diabetes. *J. Exp. Med.* 198:1103–1106.
18. Lamhamedi-Cherradi, S.E., S.J. Zheng, K.A. Maguschak, J. Peschon, and Y.H. Chen. 2003. Defective thymocyte apoptosis and accelerated autoimmune diseases in $TRAIL^{-/-}$ mice. *Nat. Immunol.* 4:255–260.
19. Rathmell, J.C., and C.B. Thompson. 2002. Pathways of apoptosis in lymphocyte development, homeostasis, and disease. *Cell.* 109:S97–S107.
20. Stassi, G., and R. De Maria. 2002. Autoimmune thyroid disease: new models of cell death in autoimmunity. *Nat. Rev. Immunol.* 2:195–204.
21. Ishimaru, N., K. Saegusa, K. Yanagi, N. Haneji, I. Saito, and Y. Hayashi. 1999. Estrogen deficiency accelerates autoimmune exocrinopathy in murine Sjogren's syndrome through Fas-mediated apoptosis. *Am. J. Pathol.* 155:173–181.
22. Ishimaru, N., R. Arakaki, M. Watanabe, M. Kobayashi, M. Miyazaki, and Y. Hayashi. 2003. Development of autoimmune exocrinopathy resembling Sjogren's syndrome in estrogen deficient mice of healthy background. *Am. J. Pathol.* 163:1481–1490.
23. Ishimaru, N., R. Arakaki, F. Omotehara, K. Yamada, K. Mishima, I. Saito, and Y. Hayashi. 2006. Novel role of RbAp48 for tissue-specific estrogen deficiency-dependent apoptosis in the exocrine glands. *Mol. Cell. Biol.* 26:2924–2935.
24. Saegusa, K., N. Ishimaru, K. Yanagi, K. Mishima, R. Arakaki, T. Suda, I. Saito, and Y. Hayashi. 2002. Prevention and induction of autoimmune exocrinopathy is dependent on pathogenic autoantigen cleavage in murine Sjögren's syndrome. *J. Immunol.* 169:1050–1057.
25. Haneji, N., T. Nakamura, K. Takio, K. Yanagi, H. Higashiyama, I. Saito, S. Noji, H. Sugino, and Y. Hayashi. 1997. Identification of α-fodrin as a candidate autoantigen in primary Sjögren's syndrome. *Science.* 276:604–607.
26. Berland, R., and H.H. Wortis. 2002. Origins and functions of B-1 cells with notes on the role of CD5. *Annu. Rev. Immunol.* 20:253–300.

27. Germain, R.N. 1994. MHC-dependent antigen processing and peptide presentation: providing ligands for T lymphocyte activation. *Cell.* 76:287–299.
28. Giroux, M., M. Schmidt, and A. Descoteaux. 2003. IFN-γ-induced MHC class II expression: transactivation of class II transactivator promoter IV by IFN regulatory factor-1 is regulated by protein kinase C-α. *J. Immunol.* 171:4187–4194.
29. Hobart, M., V. Ramassar, N. Goes, J. Urmson, and P.F. Halloran. 1997. IFN regulatory factor-1 plays a central role in the regulation of the expression of class I and II MHC genes in vivo. *J. Immunol.* 158:4260–4269.
30. Ting, J.P., and J. Trowsdale. 2002. Genetic control of MHC class II expression. *Cell.* 109:S21–S33.
31. Wright, K.L., and J.P. Ting. 2006. Epigenetic regulation of MHC-II and CIITA genes. *Trends Immunol.* 27:405–412.
32. Elser, B., M. Lohoff, S. Kock, M. Giaisi, S. Kirchhoff, P.H. Krammer, and M. Li-Weber. 2002. IFN-γ represses IL-4 expression via IRF-1 and IRF-2. *Immunity.* 17:703–712.
33. Shirasuna, K., M. Sato, and T. Miyazaki. 1981. A neoplastic epithelial duct cell line established form an irradiated human salivary gland. *Cancer.* 48:745–752.
34. Howard, A.Y. 2006. Unravelling the pros and cons of interferon-γ gene regulation. *Immunity.* 24:506–507.
35. Nakanishi, K., T. Yoshimoto, H. Tsutsui, and H. Okamura. 2001. Interleukin-18 regulates both Th1 and Th2 responses. *Annu. Rev. Immunol.* 19:423–474.
36. Bombardieri, M., F. Barone, V. Pittoni, C. Alessandri, P. Conigliaro, M.C. Blades, R. Priori, I.B. McInnes, G. Valesini, and C. Pitzalis. 2004. Increased circulating levels and salivary gland expression of interleukin-18 in patients with Sjogren's syndrome: relationship with autoantibody production and lymphoid organization of the periductal inflammatory infiltrate. *Arthritis Res. Ther.* 6:447–456.
37. Muhl, H., and J. Pfeilschifer. 2004. Interleukin-18 bioactivity: a novel target for immunopharmacological anti-inflammatory intervention. *Eur. J. Pharmacol.* 500:63–71.
38. Hurgin, V., D. Novick, and M. Rubinstein. 2002. The promoter of IL-18 binding protein: activation by an IFN-γ-induced complex of IFN regulatory factor 1 and CCAAT/enhancer binding protein-β. *Proc. Natl. Acad. Sci. USA.* 99:16957–16962.
39. Paulukat, J., M. Bosmann, M. Nold, S. Garkisch, H. Kämpfer, S. Frank, J. Raedle, S. Zeuzem, J. Pfeilschifter, and H. Mühl. 2001. Expression and release of IL-18 binding protein in response to IFN-γ. *J. Immunol.* 167:7038–7043.
40. Baccala, R., and A.N. Theofilopoulos. 2005. The new paradigm of T-cell homeostatic proliferation-induced autoimmunity. *Trends Immunol.* 26:5–8.
41. King, C., A. Ilic, K. Koelsch, and N. Sarvetnick. 2004. Homeostatic expansion of T cells during immune insufficiency generates autoimmunity. *Cell.* 117:266–277.
42. Carrasco-Marin, E., J. Shimizu, O. Kanagawa, and E.R. Unanue. 1996. The class II MHC I-Ag7 molecules from non-obese diabetic mice are poor peptide binders. *J. Immunol.* 156:450–458.
43. Rasooly, L., C.L. Burek, and N.R. Rose. 1996. Iodine-induced autoimmune thyroiditis in NOD-H-2h4 mice. *Clin. Immunol. Immunopathol.* 81:287–292.
44. Qian, Y.W., Y.C. Wang, R.E. Hollingsworth Jr., D. Jones, N. Ling, and E.Y. Lee. 1993. A retinoblastoma-binding protein related to a negative regulator of Ras in yeast. *Nature.* 364:648–652.
45. Nicolas, E., S. Ait-Si-Ali, and D. Trouche. 2001. The histone deacetylase HDAC3 targets RbAp48 to the retinoblastoma protein. *Nucleic Acids Res.* 29:3131–3136.
46. Lai, A., J.M. Lee, W.M. Yang, J.A. DeCaprio, W.G. Kaelin Jr., E. Seto, and P.E. Branton. 1999. RBP1 recruits both histone deacetylase-dependent and -independent repression activities to retinoblastoma family proteins. *Mol. Cell. Biol.* 19:6632–6641.
47. Nicolas, E., V. Morales, L. Magnaghi-Jaulin, A. Harel-Bellan, H. Richard-Foy, and D. Trouche. 2000. RbAp48 belongs to the histone deacetylase complex that associates with the retinoblastoma protein. *J. Biol. Chem.* 275:9797–9804.
48. Szende, B., I. Romics, and L. Vass. 1993. Apoptosis in prostate cancer after hormonal treatment. *Lancet.* 342:1422.
49. Spyridopoulos, I., A. Sullivan, M. Kearney, J. Isner, and D. Losordo. 1997. Estrogen-receptor-mediated inhibition of human endothelial cell apoptosis. Estradiol as a survival factor. *Circulation.* 95:1505–1514.
50. Pelzer, T., M. Schumann, M. Neumann, T. deJager, M. Stimpel, E. Serfling, and L. Neyses. 2000. 17β-estradiol prevents programmed cell death in cardiac myocytes. *Biochem. Biophys. Res. Commun.* 268:192–200.
51. Pike, C.J. 1999. Estrogen modulates neuronal Bcl-xL expression and beta-amyloid-induced apoptosis: relevance to Alzheimer's disease. *J. Neurochem.* 72:1552–1563.
52. Bouker, K.B., T.C. Skaar, D.R. Fernandez, K.A. O'Brien, R.B. Riggins, D. Cao, and R. Clarke. 2004. Interferon regulatory factor-1 mediates the proapoptotic but not cell cycle arrest effects of the steroidal antiestrogen ICI 182,780 (faslodex, fulvestrant). *Cancer Res.* 64:4030–4039.
53. Davidson, A., and B. Diamond. 2001. Autoimmune diseases. *N. Engl. J. Med.* 345:340–350.
54. Marrack, P., J. Kappler, and B.L. Kotzin. 2001. Autoimmune disease: why and where it occurs. *Nat. Med.* 7:899–905.
55. Cenci, S., G. Toraldo, M.N. Weitzmann, C. Roggia, Y. Gao, and W.P. Qian. 2003. Estrogen deficiency induces bone loss by increasing T cell proliferation and lifespan through IFN-gamma-induced class II transactivator. *Proc. Natl. Acad. Sci. USA.* 100:10405–10410.
56. Hodgin, J.B., and N. Maeda. 2002. Minireview: estrogen and mouse models of atherosclerosis. *Endocrinology.* 143:4495–4501.
57. Mikkelsen, T.R., J. Brandt, H.J. Larsen, B.B. Larsen, K. Poulsen, J. Ingerslev, N. Din, and J.P. Hjorth. 1992. Tissue-specific expression in the salivary glands of transgenic mice. *Nucleic Acids Res.* 20:2249–2255.
58. White, S.C., and G.W. Casarett. 1974. Induction of experimental autoallergic sialadenitis. *J. Immunol.* 122:178–185.
59. Saegusa, K., N. Ishimaru, K. Yanagi, R. Arakaki, K. Ogawa, I. Saito, N. Katunuma, and Y. Hayashi. 2002. Cathepsin S-inhibitor prevents autoantigen presentation and autoimmunity. *J. Clin. Invest.* 110:361–369.

Development of Inflammatory Bowel Disease in Long-Evans Cinnamon Rats Based on $CD4^+CD25^+Foxp3^+$ Regulatory T Cell Dysfunction[1]

Naozumi Ishimaru,[2]* Akiko Yamada,* Masayuki Kohashi,* Rieko Arakaki,* Tetsuyuki Takahashi,† Keisuke Izumi,† and Yoshio Hayashi*

A mutant strain with defective thymic selection of the Long-Evans Cinnamon (LEC) rat was found to spontaneously develop inflammatory bowel disease (IBD)-like colitis. The secretion of Th1-type cytokines including IFN-γ and IL-2 from T cells of mesenteric lymph node cells (MLNs) and lamina propria mononuclear cells, but not spleen cells, in LEC rats was significantly increased more than that of the control Long-Evans Agouti rats through up-regulated expression of T-bet and phosphorylation of STAT-1 leading to NF-κB activation. In addition, the number of $CD4^+CD25^+Foxp3^+$ regulatory T (Treg) cells of the thymus, MLNs, and lamina propria mononuclear cells from LEC rats was significantly reduced, comparing with that of the control rats. Moreover, bone marrow cell transfer from LEC rats into irradiated control rats revealed significantly reduced $CD25^+Foxp3^+$ Treg cells in thymus, spleen, and MLNs compared with those from control rats. Indeed, adoptive transfer with T cells of MLNs, not spleen cells, from LEC rats into SCID mice resulted in the development of inflammatory lesions resembling the IBD-like lesions observed in LEC rats. These results indicate that the dysfunction of the regulatory system controlled by Treg cells may play a crucial role in the development of IBD-like lesions through up-regulated T-bet, STAT-1, and NF-κB activation of peripheral T cells in LEC rats. *The Journal of Immunology,* **2008, 180: 6997–7008.**

Inflammatory bowel disease (IBD)[3] in humans has two manifestations including Crohn's disease and ulcerative colitis (1–3). Although the precise mechanisms of the diseases are unknown, it has been reported that activation of the intestinal immune system in response to bacterial Ags with pathologic cytokine production of intestinal T cells through various transcription factors or signal molecules such as T-bet, GATA-3, and STATs plays a key role in the pathogenesis of IBD (4–7). The cytokine production by T cells is known to initiate and develop chronic intestinal inflammation (8–10). Crohn's disease is associated with Th1 cytokines such as IFN-γ and TNF-α (11, 12). Meanwhile, ulcerative colitis in human is associated with Th2 cytokine such as IL-5 (13). In addition, it is suggested that Th3 cytokine such as TGF-β has the immunosuppressive effect of IBD in human and animal models (14, 15). Furthermore, it is reported that nucleotide-binding oligomerization domain-containing proteins expressed in intestinal epithelial cells or APCs play a crucial role in the Th1 response in Crohn's disease (16–19). However, the pathogenesis based on cytokine balance of peripheral T cells for IBD is still unclear.

$CD4^+CD25^+$ regulatory T (Treg) cells have been widely studied in controlling inflammatory diseases including IBD (20–23). It is well known that the IBD model, by transfer of naive $CD45RB^{high}CD4^+$ T cells into T cell-deficient mice, can be controlled by coinjection of Treg cells to suppress $CD4^+$ effector T cell functions such as IFN-γ production (24). It has been reported that the cell number of Treg in the periphery from IBD patients was significantly reduced, or soluble IL-2Rα (CD25) of sera from IBD patients was increased (25, 26). However, it is obscure how natural Treg cells generated from thymus influence the pathogenesis of IBD.

Many animal models—such as C3H/HeJBir, IL-2-deficient, IL-2R-deficient, and IL-10-deficient mice, and HLA-B27/β2 transgenic rats—are known to be referred to as human IBD (27–31). It has been reported that the disease is induced by the hyperresponsiveness of T cells which is shifted to Th1 or Th2 cytokine production in each model (11–13). Cytokines produced by lamina propria (LP) $CD4^+$ T lymphocytes appear to initiate and perpetuate chronic intestinal inflammation. It is also reported that Th1 or Th2 cytokine production in IBD models can be modulated by the immunosuppressive cytokine such as TGF-β secreted by Th3 cells (22, 23). In addition, some transcription factors including T-bet and GATA-3 or signal molecules such as STATs are well known to regulate immunopathogenic or immunosuppressive cytokine production for controlling IBD (7).

The Long-Evans Cinnamon (LEC) rat was first described to be a naturally occurring mutant with a specific defect in thymocyte development, which has contained T cell differentiation arrest

*Department of Oral Molecular Pathology, Institute of Health Biosciences, University of Tokushima Graduate School, Kuramotocho, Tokushima, Japan; and †Department of Molecular and Environmental Pathology, Institute of Health Biosciences, University of Tokushima Graduate School, Kuramotocho, Tokushima, Japan

Received for publication August 24, 2007. Accepted for publication March 13, 2008.

The costs of publication of this article were defrayed in part by the payment of page charges. This article must therefore be hereby marked *advertisement* in accordance with 18 U.S.C. Section 1734 solely to indicate this fact.

[1] This work was supported in part by Grants-in-Aid for Scientific Research (17109016 and 17689049) from the Ministry of Education, Culture, Sports, Science, and Technology of Japan.

[2] Address correspondence and reprint requests to Dr. Naozumi Ishimaru, Department of Oral Molecular Pathology, Institute of Health Biosciences, University of Tokushima Graduate School, 3-18-15 Kuramotocho, Tokushima 770-8504, Japan. E-mail address: ishimaru@dent.tokushima-u.ac.jp

[3] Abbreviations used in this paper: IBD, inflammatory bowel disease; Treg, regulatory T; DP, double positive; SP, single positive; MLN, mesenteric lymph node cell; LP, lamina propria; BM, bone marrow; PAS, periodic acid Schiff; DAPI, 4′,6-diamidino-2-phenylindole; HPRT, hypoxanthine phosphoribosyltransferase; LPMC, LP mononuclear cell.

from $CD4^+CD8^+$ double-positive (DP) to $CD4^+CD8^-$ single-positive (SP) but not to $CD4^-CD8^+$ SP thymocytes (32). In addition, peripheral $CD4^+$ T cells of LEC rats were shown not to function as Th cells in Ab production against T cell-dependent Ag and IL-2 production by polyclonal stimulation (32, 33). However, it remains unclear whether the T cell dysfunction of LEC rats might have an influence on any disease associated with the immune disorder. In the present study, we found for the first time that IBD-like lesions developed spontaneously in LEC rats. Thus, the pathogenesis and molecular mechanisms of inflammatory bowel lesions in LEC rats as a human IBD model were analyzed.

Materials and Methods

Animals

LEC rats and LEA rats as controls were maintained in our laboratory under specific pathogen-free conditions. SCID mice (C.B-17/*Icr-scid/scid Jcl*) were purchased from CLEA Japan for use as recipients of adoptive transfer. The experiments were approved by an animal ethics board of Tokushima University.

Pathological analysis

All organs of rats and recipient mice were removed and fixed in 10% phosphate-buffered formaldehyde (pH 7.2), embedded in paraffin, and prepared for histological estimation. The sections were stained with H&E. The disease incidence was evaluated by three independent, well-trained pathologists in a blinded manner.

Flow cytometric analysis

Surface markers on lymphocytes from thymus, spleen, mesenteric lymph node cells (MLNs), and LP were analyzed by using an EPICS flow cytometer (Beckman Coulter) using FITC-, PE-Cy5-, or PE-conjugated anti-CD4, -CD8, -CD44, -CD62L, and -CD25 mAbs (BD Biosciences). To evaluate intracellular Foxp3 expression, lymphocytes were stained with anti-CD4 and -CD25 mAb, fixed and permeabilized with the buffers of a Foxp3 detection kit (BD Biosciences). After staining with anti-Foxp3 mAb, the lymphocytes were analyzed by flow cytometry.

Proliferation assay

T cells (>90%) were enriched from single-cell suspensions of spleen and lymph node cells from LEC, control rats, and SCID mice with nylon wool (Wako Pure Chemical), and cultured in 96-well flat-bottom microtiter plates (5×10^4 cells/well) in RPMI 1640 containing 10% FCS, penicillin/streptomycin, and 2-ME. Cells were stimulated with plate-coated anti-CD3 (BD Biosciences) and anti-CD28 mAb (BD Biosciences). [^{3}H]Thymidine incorporation during the last 12 h of the culture for 72 h was evaluated using an automated β liquid scintillation counter. In addition, to detect cell proliferation of the T cell subset, after CFSE (Molecular Probes)-labeled T cells were cultured for 48 h, the T cells were stained with anti-CD4 and -CD8 mAb. Cell divisions of $CD4^+$- or $CD8^+$-gated T cells were analyzed by flow cytometry. For T cell suppression assay, $CD25^-CD4^+$ or $CD25^+CD4^+$ T cells of MLN from control or LEC rats were enriched using biotin-conjugated anti-CD25 mAb, anti-CD4 mAb (BD Biosciences), magnetic beads, and the CELLection Biotin Binder kit (Dynal Biotech). A total of 5×10^4 $CD25^-CD4^+$ T cells from control rats were stimulated with plate-coated anti-CD3 mAb (0.5 μg/ml) for 72 h together with 0, 0.625, 1.25, and 2.5×10^4 $CD25^+CD4^+$ T cells from control or LEC rats. [^{3}H]Thymidine incorporation during the last 12 h of the culture was evaluated using an automated β liquid scintillation counter.

ELISA

Cytokine production was tested by a solid-phase sandwich ELISA using a rat IL-2, IL-4, IFN-γ, and IL-10 kit (BioSource International). In brief, culture supernatants from T cells from lymph nodes or spleen stimulated with anti-CD3 and -CD28 mAbs for 24 h and were added to microtiter plates precoated with an each Ab specific for rat L-2, IL-4, IFN-γ, and IL-10. The biotinylated Ab was added and the plate was incubated for 2 h at room temperature. After washing, streptavidin-HRP solution was added to each well and the plate was incubated for 30 min at room temperature. Finally, stabilized chromogen substrate was added to each well, and the absorbance of each well was read at 450 nm using an automatic microplate reader (Bio-Rad). The concentrations of cytokines were obtained according to the standard curves.

Western blot analysis

Isolated T or $CD4^+$ T cells from spleen and lymph nodes using nylon wool (Wako Pure Chemical) or PE-conjugated CD4 mAb with a magnetic PE selection kit (StemCell Technologies) were stimulated with anti-CD3/-CD28 mAbs for 12~24 h, washed, pelleted, and incubated in 20 mM/L Tris-HCl (pH 8.0), 20 mM/L NaCl, 0.5% Triton X-100, 5 mM/L EDTA, and 3 mM/L $MgCl_2$ lysis buffer including protease inhibitor mixture (Sigma-Aldrich). After centrifugation for 20 min at 12,000 rpm, supernatant was extracted and used as whole cell lysates. The nuclear extracts were purified using a Nuclear/Cytosol Fraction kit (BioVision). A total of 5~20 μg of each sample per well was applied for each well and electrophoresed in 10% SDS-polyacrylamide gel. Then, the protein was electrophoretically transferred to polyvinylidene difluoride membrane. The membrane was incubated with anti-T-bet, -GATA-3, -STAT-1, -phospho-STAT1, -GAPDH, -histone (Santa Cruz Biotechnology), and -Foxp3 (eBioscience) as the primary Abs. HRP-conjugated rabbit or mouse IgG was used as the second Ab. Protein binding was visualized with ECL Western blotting reagent (Amersham Biosciences). To quantify the protein expression, the chemiluminescence image was analyzed by ChemiDoc XRS (Bio-Rad).

Cell transfer

Bone marrow cells (5×10^6) from LEC and control rats were transferred i.v. into irradiated (4 Gy) control rats. Four weeks after the transfer, the host rats were analyzed. As for adoptive transfer to induce IBD-like lesions, purified T cells (5×10^6) from MLNs or spleen cells of LEC and control rats with nylon wool (Wako Pure Chemical) as donors were used and transferred i.p. into SCID mice. Six weeks after the transfer, the recipient SCID mice were sacrificed and all organs were histologically analyzed. In addition, MLN cells of SCID mice were cultured, and cytokine productions of the supernatants of the cells were analyzed by ELISA.

Injection of neutralizing Abs

A total of 50 μg of anti-rat IFN-γ mAb (PBL Biomedical Laboratories), anti-rat IL-4 mAb (R&D Systems), anti-rat CD8 mAb (BD Biosciences), and isotype control Ab were injected i.v. twice a week into LEC rats from 8 to 10 wk of age. Colon sections were stained with H&E and periodic acid Schiff (PAS), and the pathology was scored blindly using a semiquantitative scale of 0–5 as described previously (34). In summary, grade 0 was assigned when no changes were observed; grade 1, minimal inflammatory infiltrates present in the LP with or without mild mucosal hyperplasia; grade 2, mild inflammation in the LP with occasional extension into the submucosa, focal erosions, minimal to mild mucosal hyperplasia and minimal to moderate micin depletion; grade 3, mild to moderate inflammation in the LP and submucosa occasionally transmural with ulceration and moderate mucosal hyperplasia and mucin depletion; grade 4, marked inflammatory infiltrates commonly transmural with ulceration, marked mucosal hyperplasia and mucin depletion, and multifocal crypt necrosis; grade 5, marked transmural inflammation with ulceration, widespread crypt necrosis, and loss of intestinal glands.

Immunofluorescence staining and confocal microscopic analysis

Frozen sections of colon from LEC and control rats were fixed with 3% paraformaldehyde in PBS, and preblocked with 1% BSA-2.5% FCS in PBS for 1 h. Sections were stained with 1 μg/ml of primary Abs against CD4, CD8, CD45R, CD11b/c (BD Biosciences), T-bet, NF-κB, GATA-3, and phospho-STAT1 (Santa Cruz Biotechnology) for 1 h. After three washes in PBS, the sections were stained with Alexa Fluor 488 donkey anti-mouse IgG (H+L) or goat anti-rabbit IgG (H+L) (Molecular Probe) as the second Abs for 30 min and washed with PBS. The section stained with intracellular proteins were stained with PE-labeled anti-CD4 mAb. The nuclei was stained with 4′,6-diamidino-2-phenylindole (DAPI). The sections were visualized with a laser scanning confocal microscope (Carl Zeiss). A 63 × 1.4 oil differential interference contrast objective lens was used. Quick Operation Version 3.2 (Carl Zeiss) for imaging acquisition and Adobe Photoshop CS2 (Adobe Systems) for image processing were used.

Real-time quantitative RT-PCR

Total RNA was extracted from purified lymphocytes of the thymus, spleen, and MLNs in LEC and control rats using Isogen (Wako Pure Chemical), and was reverse transcribed as described (35). Transcript levels of Foxp3 and hypoxanthine phosphoribosyltransferase (HPRT) were performed using PTC-200 DNA Engine Cycler (MJ Research) with SYBR Premix Ex Tag (Takara). The primer sequences were as follows: Foxp3: forward, 5′-CCCAGGAAAGACAGCAACCTT-3′ and reverse, 5′-CTGCT TGGCAGTGCTTGAGAA-3′; and HPRT: forward, 5′-TGTTGGATACAG

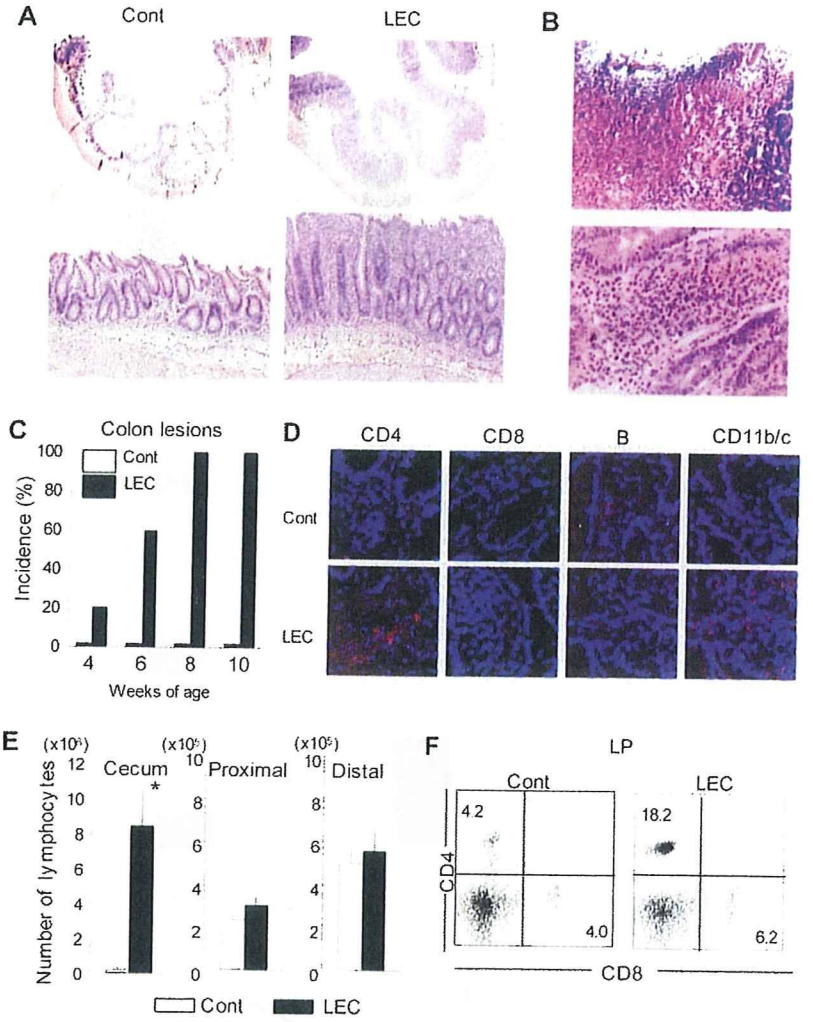

FIGURE 1. IBD-like lesion of LEC rats. *A*, Pathology of colon lesions from LEC and control rats. The thickened wall of colon was found in LEC rats. Inflammatory findings with lymphocyte infiltration were observed in cecum sections from LEC, not control rats, at 8 wk of age. Representative photomicrographs (original magnification, ×20 and 100) of H&E-stained paraffin section from LEC and control rats are shown. *B*, Development of IBD-like lesions of LEC rats. Ulceration and mononuclear cell infiltration was found in the colon lesions of LEC rats. Representative photomicrographs (original magnification, ×100 and 200) of H&E-stained paraffin section of colon from LEC rats are shown. *C*, Incidence of IBD-like lesions in LEC rats. The incidence of IBD-like lesions of LEC and control rats at 4–10 wk of age was evaluated by histological analysis. Complete absence of colon lesions in control rats was found. Approximately four to nine rats were analyzed for each age. *D*, Immunohistochemical analysis of infiltrating cells into colon lesions of LEC rats. Staining with anti-CD4, -CD8, -CD45R, and -CD11b/c was performed using the sections from LEC and control rats at 8 wk of age. Alexa 568 (red) as the second Ab and DAPI (blue) for nuclear staining was used. Photos are representative of three to five samples (original magnification, ×630). *E*, The number of LP lymphocytes in cecum, proximal, and distal colon tissues from LEC and control rats was evaluated. The number of cells was shown as mean (percent) ± SD from five to eight rats in each group. *, $p < 0.0005$ LEC vs control rats. *F*, T cell subsets of LP lymphocytes in the lesions of LEC rats. Flow cytometric analysis was performed with LP lymphocytes of cecum from LEC and control rats of 8 wk of age. A representative result of five samples is shown.

GCCAGACTTTGT-3′ and reverse, 5′-TCCACTTTCGCTGATGAC ACA-3′. Results were calculated by a software of DNA Engine Opicon System (Roche Molecular System).

Statistics

The Student *t* test was used for statistical analysis. Values of $p > 0.05$ were considered significant.

Results

Pathology of colon lesion of LEC rats

Histopathological analysis of all organs of LEC rats from 4 to 12 wk of age was performed. Thickened LP of the colon from LEC rats was observed relative to that from control LEA rats (Fig. 1*A*). Ulcer formation with fibrin exudates, mononuclear cell, and neutrophil infiltration was observed in the surface of the lesion (Fig. 1*B*, *upper*). In the thickened LP of LEC rats, mononuclear cell infiltration was prominent (Fig. 1*B*, *lower*). Most severe inflammatory lesions were seen in the tissue around the cecum in LEC rats. Although the precise mechanisms as to why the most severe lesion developed in the tissue around the cecum of LEC rats is unclear, it is possible that the differential bacterial distribution from the other segments of colon or unique mucosal immunity of cecum may influence the cecum lesion of LEC rats. No inflammatory lesions in LEC rats were observed in the other organs in general. The colon lesions developed spontaneously in almost 100% of LEC rats at 8 wk of age or more, and the incidence of lesions was consistently increased with aging (Fig. 1*C*). There was no sex difference in the colon lesions of LEC rats. LEC rats have also been reported as an animal model for Wilson's disease because of the genetic copper metabolism disorder (36). It is known that the body weight of LEC rats is significantly reduced compared with that of control rats because of the disease (37). Therefore, it is unclear whether the IBD-like lesions of the LEC rat may influence the loss of body weight.

To clarify the population of the immune cells infiltrated in the LP of IBD-like lesions from LEC rats, immunohistochemical analysis was performed using the cecum sections from LEC rats. We found that $CD4^+$ T cells and $CD11b/c^+$ macrophages or dendritic cells were mainly infiltrated, and a small number of $CD45R^+$ B and $CD8^+$ T cells were also found in the lesions of LEC rats (Fig. 1*D*). The total cell number of lymphocytes in the LP of cecum among colon from LEC rats was significantly higher than that from control rats (Fig. 1*E*). However, there was no difference in number of LP mononuclear cells (LPMCs) in proximal and distal colon between control and LEC rats (Fig. 1*E*). Moreover, flow cytometric analysis with T lymphocytes in the LP of the lesions revealed that the prominent population was $CD4^+$ T cells compared with those of control rats (Fig. 1*F*).

Characteristics of T cells from LEC rats

To examine the immunological characteristics in LEC rats, the thymocytes and peripheral T cells were analyzed. We found that

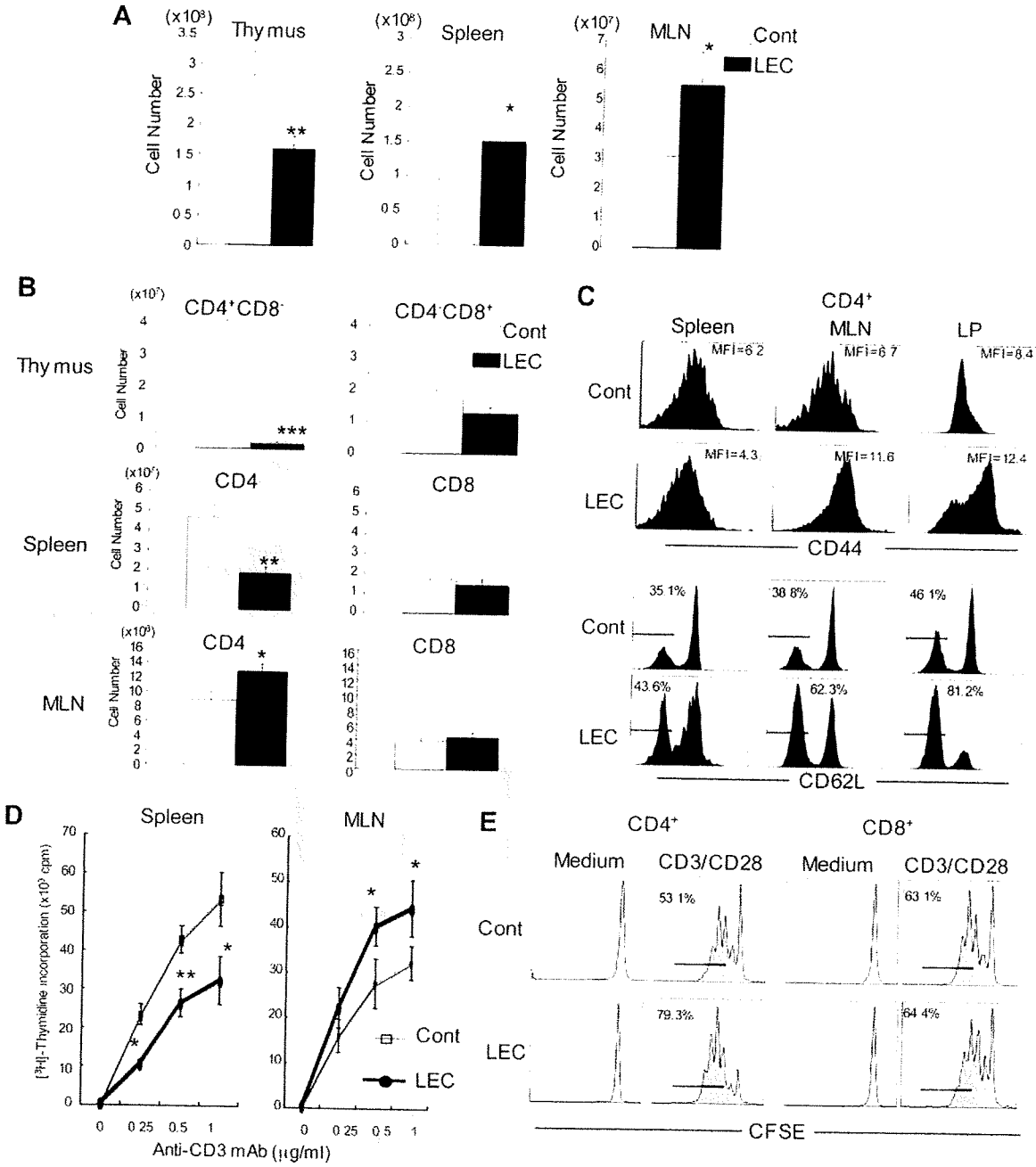

FIGURE 2. Characteristics of T cells from LEC rats. *A*, The cell number of the thymus, spleen, and MLNs are shown as mean ± SD from five to seven LEC and control rats of at 2 mo of age. *, $p < 0.05$; **, $p < 0.0005$ LEC vs control rats. *B*, T cell subsets of the thymus, spleen, and MLNs from LEC rats. Flow cytometric analysis was performed using thymocytes, spleen cells, and MLN cells. The number of $CD4^+$ or $CD8^+$ T cells was shown as mean (percent) ± SD from five to eight rats in each group. *, $p < 0.0005$; **, $p < 0.00005$; ***, $p < 0.0000005$ LEC vs control rats. *C*, Activation of $CD4^+$ T cells from LEC rats. CD44 and CD62L expressions on $CD4^+$ T cells of spleen and MLNs from control and LEC rats were analyzed by flow cytometric analysis. Mean fluorescence intensity (MFI) of CD44 expression is shown. $CD62L^-$ cells (percent) are indicated in the panels. Results are representative of three samples. *D*, Proliferative responses were analyzed by [^{3}H]thymidine incorporation using spleen and MLN T cells stimulated with plate-coated CD3 mAb (0~1 μg/ml) and CD28 mAb (5 μg/ml) for 72 h. The data are shown as the mean ± SD of three triplicate samples. Graphs are representative of three independent experiments. *, $p < 0.05$; **, $p < 0.005$ LEC vs control rats. *E*, Purified T cells from MLNs of control and LEC rats were labeled with CFSE (0.5 μM), and stimulated with CD3 mAb (1 μg/ml) and CD28 mAb (5 μg/ml) for 72 h. CFSE dilution of $CD4^+$ and $CD8^+$ T cells was estimated by flow cytometry. Graphs are representative of three independent experiments.

the cell number of thymus and spleen from LEC rats was significantly lower than that from control rats, while the cell number of MLNs was significantly higher compared with that from control rats (Fig. 2*A*). Significant reduction of $CD4^+CD8^-$ cells of the thymus and $CD4^+$ T cells of the spleen from LEC rats was observed in contrast to the populations from control rats as described in the previous report (Fig. 2*B*) (32). In contrast, there was a greater increase of $CD4^+$ T cell number of MLNs found in LEC rats compared with that from control rats (Fig. 2*B*). No significant change for $CD8^+$ T cells was observed in the thymus, spleen, and MLNs (Fig. 2*B*). In addition, CD44 expression, one of the activation markers for T cells, on $CD4^+$ T cells of MLNs and LP from LEC rats was significantly higher than that from control rats (Fig. 2*C*). Also, $CD62L^-CD4^+$ T cells, which are memory phenotype,

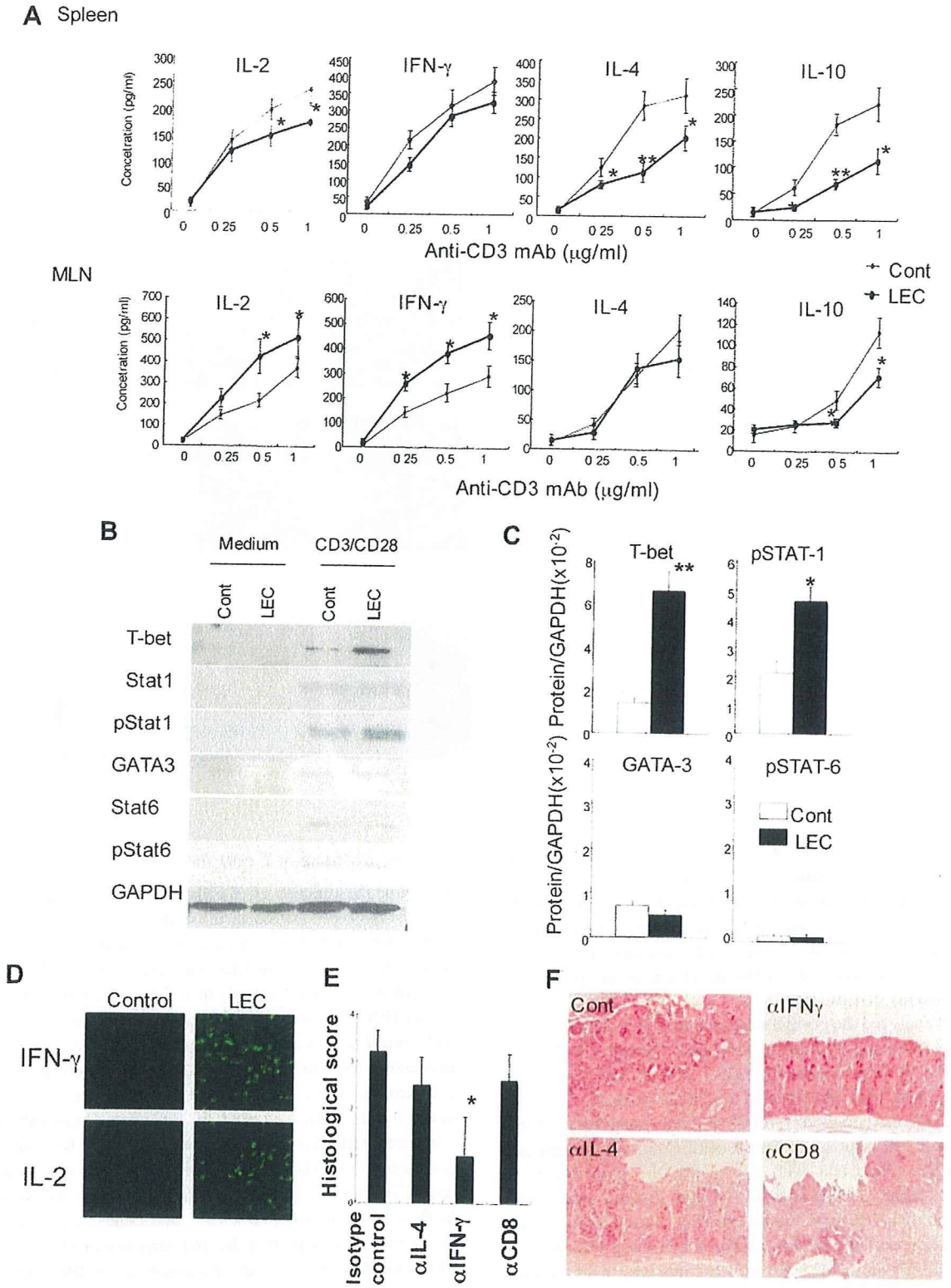

FIGURE 3. Cytokine switching of LEC rats. *A*, Purified T cells of the spleen and MLNs from LEC and control rats were stimulated with CD3 mAb (0~1 μg/ml) and CD28 mAb (5 μg/ml) for 24 h. The culture supernatants were analyzed for cytokine productions including IL-2, IFN-γ, IL-4, and IL-10 by ELISA. The concentration was shown as the mean ± SD of three triplicate samples. Graphs are representative of two independent experiments. *, $p < 0.05$; **, $p < 0.005$ LEC vs control rats. *B*, Purified T cells of MLNs from control and LEC rats were stimulated with CD3-CD28 ligation for 24 h. The cell lysates were used for the expression of T-bet and GATA-3, and the expression and phosphorylation of STAT-1 and STAT-6. GAPDH was used as a housekeeping protein. The photos are shown as representative results from three samples. *C*, Protein quantification of cytokine-switching molecules was performed using chemiluminescence images. Relative expressions to GAPDH were calculated. Results are mean ± SD of three samples. *, $p < 0.05$; **, $p < 0.005$ LEC vs control rats. *D*, IFN-γ and IL-2 expressions of colon were detected by immunofluorescence staining with the first mAbs and Alexa 488-conjugated anti-mouse IgG as the second Ab. The photos are shown as representative results from three samples. *E*, The neutralizing mAbs (50 μg/rat) and isotype control Ab (50 μg/rat) were i.v. injected twice a week into LEC rats from 8 to 10 wk of age. Colonic histology scores of experimental rats are shown. Data are mean ± SD of four to six rats per group. *, $p < 0.05$ treated vs control Ab treated. *F*, Sections of colons from neutralizing Ab-treated LEC rats were stained with PAS. Photos are representative of each group.

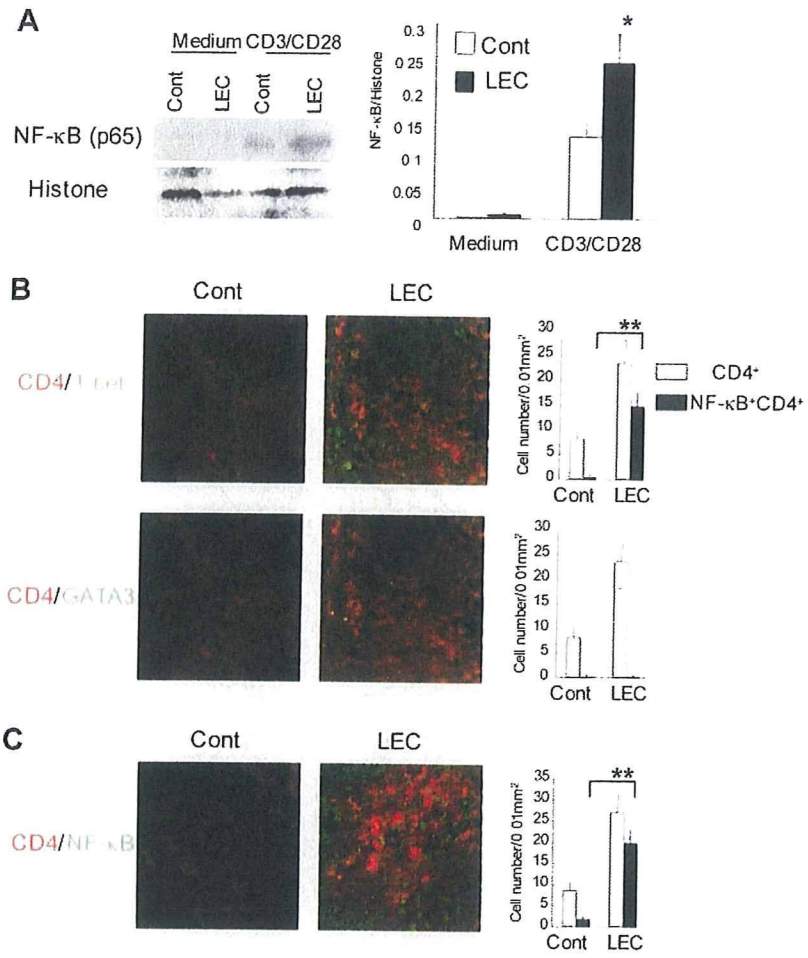

FIGURE 4. NF-κB activation of T cells in the IBD-like lesions from LEC rats. *A*, NF-κB activation of T cells from LEC rats. Purified MLN T cells were stimulated with CD3-CD28 ligation for 24 h, and the expressions of NF-κB (p65) and histone as a housekeeping protein in the nuclear extracts were tested by Western blotting. Relative expression of NF-κB to histone was calculated. Photos are representative and data are mean ± SD of three independent experiments. *B* and *C*, Confocal analysis of T-bet, GATA-3, and NF-κB of infiltrating $CD4^+$ T cells in IBD-like lesions from LEC and control rats. Frozen sections were stained with Alexa 488-labeled T-bet, GATA-3, or NF-κB (green), and Alexa 568-labeled CD4 (red). Photos are shown as representative of three samples. Data are mean ± SD of cell number ($CD4^+$ or $NF\text{-}\kappa B^+CD4^+$) per 0.01 mm^2 of five independent areas. **, $p < 0.005$ control vs LEC rats.

of MLNs and LP from LEC rats were significantly increased compared with those from control rats (Fig. 2*C*). As for CD69 expression, one of early activation markers, there was no difference between control and LEC rats (data not shown). These findings strongly suggest that $CD4^+$ T cells of MLNs and LP from LEC rats may play a crucial role in the development of spontaneous IBD-like lesions of LEC rats.

We next analyzed the proliferative response of T cells from LEC and control rats using stimulation with anti-CD3 and -CD28 mAbs. Purified T cells from spleen and MLNs of LEC and control rats were stimulated with plate-coated anti-CD3 mAb (0~1 μg/ml) and anti-CD28 mAb (5 μg/ml) for 72 h. It was previously reported that splenic T cell response to Con A of LEC rats was significantly reduced (32). Consistent with the report, the proliferative responses of splenic T cells with CD3-CD28 ligation were significantly lower than that from control rats (Fig. 2*D*). However, it was interesting to note that a prominent increase in T cell response with CD3-CD28 ligation in MLNs from LEC rats was observed compared with that from control rats (Fig. 2*D*). To clarify which population of T cells indicates higher proliferative response, the purified T cells of MLNs were labeled with CFSE, and stimulated with CD3-CD28 ligation for 72 h. Proliferative response of $CD4^+$ or $CD8^+$ T cells was analyzed by flow cytometry using CFSE dilutions. We found that $CD4^+$ T cells of MLNs from LEC rats were clearly much more proliferative compared with those from control rats, whereas no difference was observed in $CD8^+$ T cells between LEC and control rats (Fig. 2*E*). These results indicate that the $CD4^+$ T cells in MLNs from LEC rats are primarily responsible for the development of IBD-like lesions in LEC rats.

Cytokine switching of T cells in LEC rats

To define the function of T cells of spleen and MLNs from LEC rats, cytokine production in the culture supernatants from T cells stimulated with CD3-CD28 ligation was analyzed. IL-2 production in the spleen cells from LEC rats was significantly lower (anti-CD3 mAb: 0.5 and 1 μg/ml) than those in control rats (Fig. 3*A*). As for IFN-γ in spleen, no difference was observed between LEC and control rats. In addition, a significant decrease in Th2 cytokine production including IL-4 and IL-10 was observed in the spleen cells from LEC rats. In contrast, Th1 cytokines (IL-2 and IFN-γ) in the T cells of MLNs from LEC rats were significantly increased compared with those in control rats (Fig. 3*A*). By contrast, IL-10 production from MLN T cells in LEC rats was significantly lower (anti-CD3 mAb: 1 μg/ml) than that in control rats. No difference in IL-4 production between LEC and control rats was observed. These results indicate that the Th1 response of MLN T cells from LEC rats may influence the pathogenesis of IBD-like lesions in LEC rats.

It is well known that T-bet and GATA-3 are key transcription factors in controlling Th1 or Th2 cytokine production (4, 5). We then analyzed the expression T-bet and GATA-3 using the T cells of MLNs stimulated with CD3-CD28 ligation. T-bet expression of T cells from LEC rats was relatively increased comparing with that from control rats, whereas no difference in GATA-3 expression was observed between LEC and control rats (Fig. 3*B*). Moreover, the expression of STAT-1 and STAT-6, which exist upstream of T-bet and GATA-3, respectively, was analyzed. Increased phosphorylation of STAT-1 in T cells of MLNs from LEC rats was

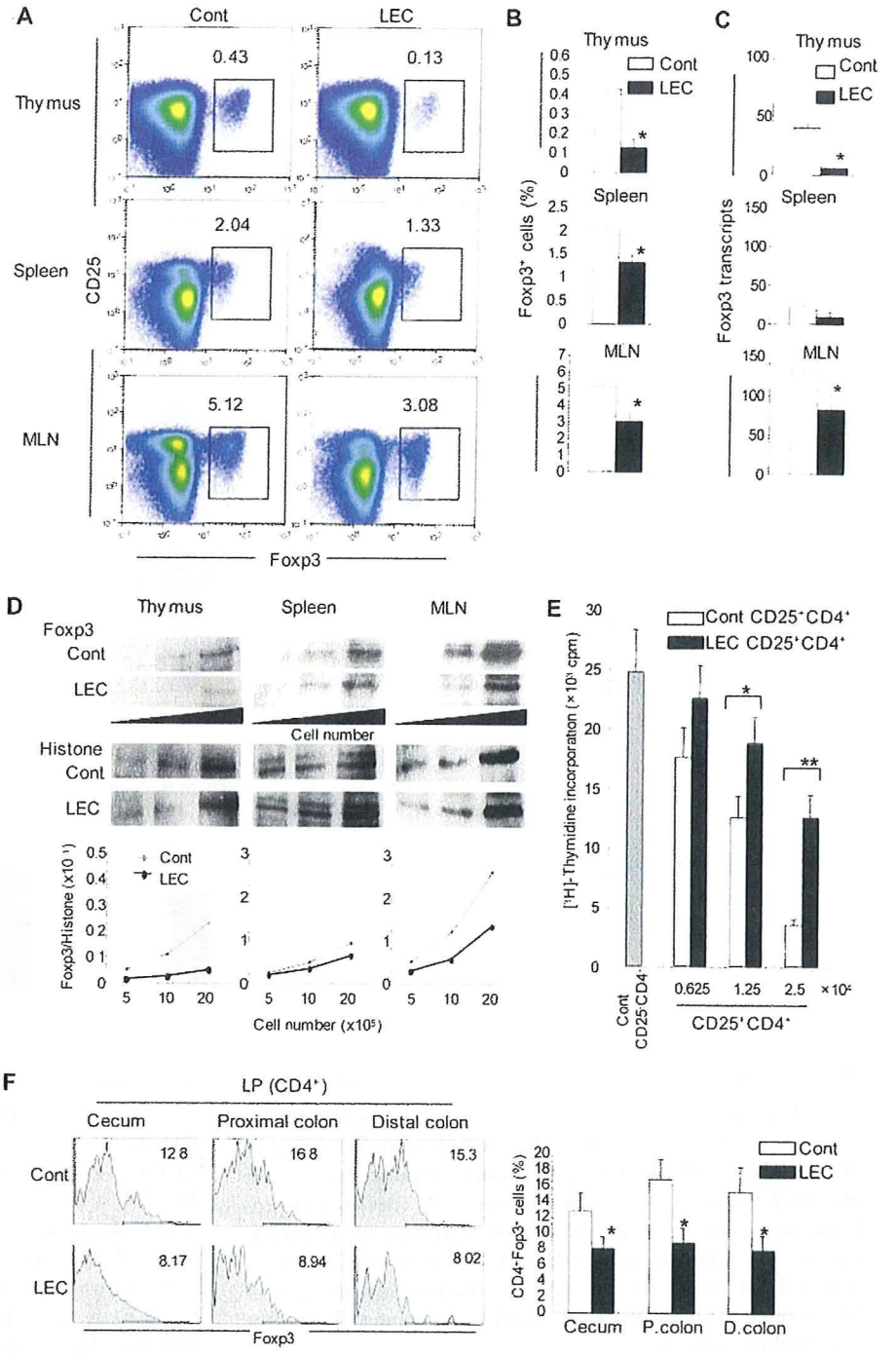

FIGURE 5. $CD25^+Foxp3^+CD4^+$ T cells in LEC rats. *A*, $CD25^+Foxp3^+CD4^+$ T cells in the thymus, spleen, and MLNs from LEC and control rats were analyzed by flow cytometry. Graphs are representative of three samples. *B*, $CD25^+Foxp3^+CD4^+$ T cells (percent) were shown as mean ± SD of three samples. *, $p < 0.05$; **, $p < 0.005$; ***, $p < 0.0005$ LEC vs control rats. *C*, The mRNA expression of Foxp3 in LEC rats. The expressions of the thymus, spleen, and MLNs were tested by real-time quantitative RT-PCR. Relative Foxp3 transcripts to HPRT were shown as mean ± SD of three samples. *, $p < 0.05$ LEC vs control rats. *D*, The Foxp3 expression of the nuclear extracts of 0.5×10^6, 1×10^6, and 2×10^6 $CD4^+$ T cells was confirmed by Western blotting. Histone was used as a housekeeping protein. Protein quantification of Foxp3 was performed using chemiluminescence images. Relative Foxp3 expression to histone of the nuclear extracts of 0.5×10^6, 1×10^6, and 2×10^6 T cells was estimated. Results are representative of three samples. *E*, A total of 5×10^4 $CD25^-CD4^+$ T cells of MLN from control rats were cocultured with 0.625–2.5×10^4 $CD25^+CD4^+$ T cells of MLNs from control or LEC rats on anti-CD3 mAb-coated plate. Data are mean ± SD of triplicates, representative of three independent experiments. *, $p < 0.05$; **, $p < 0.005$ control $CD25^+CD4^+$ vs LEC $CD25^+CD4^+$. *F*, Foxp3 expression of $CD4^+$ LPMCs in cecum, proximal, and distal colon from control and LEC rats was detected. Results are representative of four to six rats. Data are mean ± SD of $CD4^+Foxp3^+$ cells (percent) of four to six rats. *, $p < 0.05$ control vs LEC rats.

detected, but no difference was observed in STAT-1 expression between LEC and control rats. By contrast, there was no difference in the expression and phosphorylation of STAT-6 in either group (Fig. 3*B*). To quantify the protein expressions of T-bet, pStat-1, GATA-3, and pSTAT-6, relative expressions to GAPDH as a housekeeping protein were shown in Fig. 3*C*. T-bet expression of stimulated MLN T cells from LEC rats was 4~5-fold higher compared with that of control rats. The pSTAT-1 had an expression that was twice as high relative to that of control rats. Furthermore, increased expression of Th1 cytokines including IL-2 and IFN-γ of $CD4^+$ T cells in LP from LEC rats was observed compared with that from control rats by fluorescence staining (Fig. 3*D*). By contrast, IL-4- or IL-10-producing cells were undetectable in the LP from both control and LEC rats (data not shown). To examine the correlation of Th1 cytokine with colitis of LEC rats, anti-IFN-γ-neutralizing Ab, anti-IL-4-neutralizing Ab, or isotype control Ab was injected into LEC rats from 8 to 10 wk of age, and the histology of colitis was evaluated (Fig. 3*E*). Histological score of LEC rats administrated with anti-IFN-γ mAb was significantly lower than that with isotype control Ab. No significant change was observed by injection of anti-IL-4 mAb. Moreover, to investigate the role of $CD8^+$ T cells in the development of colitis, anti-CD8-neutralizing Ab to deplete $CD8^+$ T cells was injected into LEC rats. There was no significant change of pathology in anti-CD8 mAb administered LEC rats, compared with that in controls (Fig. 3*E*). Ulcer formation, lymphocyte infiltrates, decreased numbers of mucin-producing cells, and mucosal hyperplasia were observed in the sections from isotype control Ab, anti-IL-4 mAb, and anti-CD8 mAb-injected rats, while injection of anti-IFN-γ mAb was able to effectively suppress the colon lesion of LEC rats (Fig. 3, *E* and *F*).

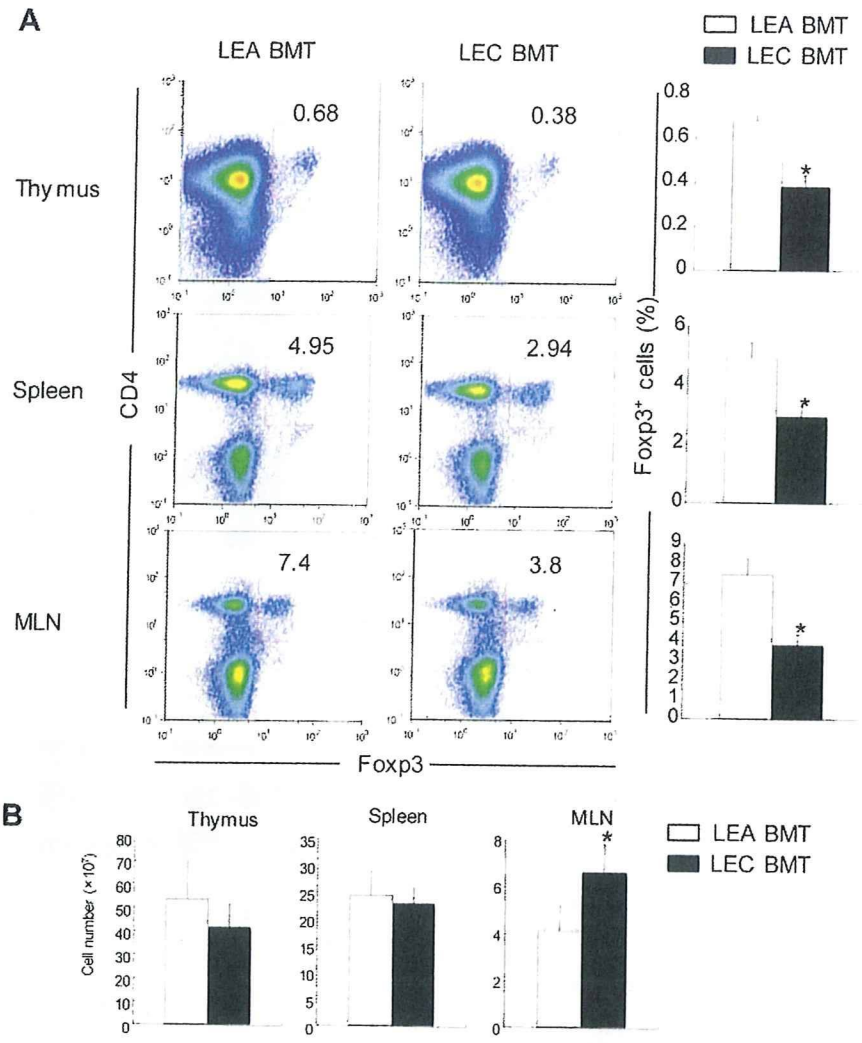

FIGURE 6. *A*, The generation of Treg cells from BM cells in LEC rats. A total of 5×10^6 BM cells from LEA or LEC rats were i.v. transferred into irradiated (4 Gy) LEA rats. At 4 wk after transfer, intracellular Foxp3 expression of $CD4^+CD25^+$ cells in thymus, spleen, and MLNs from the chimeric rats were analyzed by flow cytometry. Results are representative of three mice, and data are shown as the mean ± SD of three rats. *, $p < 0.05$ LEA BMT vs LEC BMT recipients. *B*, Total cell number in thymus, spleen, and MLN from LEA BMT and LEC recipient rats were counted with trypan blue staining. Data are mean ± SD of three rats. *, $p < 0.05$ LEA BMT vs LEC BMT.

NF-κB activation of T cells in IBD-like lesions from LEC rats

To further confirm whether the T cell signal via up-regulated T-bet and phosphorylation STAT-1 in MLN T cells from LEC rats can lead to NF-κB activation, which is a potent transcription factor regulating the target genes essential for T cell activation or proliferation (38–41), we analyzed NF-κB expression of the nuclear extracts of T cells stimulated with CD3-CD28 ligation. We demonstrated that there was an increased nuclear translocation of NF-κB (p65) of stimulated T cells in LEC rats compared with that in control rats (Fig. 4*A*).

We next examined the expression of T-bet, GATA-3, and nuclear translocation of NF-κB of infiltrating $CD4^+$ T cells in IBD-like lesions from LEC rats by confocal microscopy. Increased expression of T-bet together with nuclear transport of NF-κB was observed in $CD4^+$ T cells of inflammatory lesions from LEC rats (Fig. 4, *B* and *C*), whereas GATA-3^+ $CD4^+$ T cells were almost undetectable in the lesions (Fig. 4*B*). These results imply that T cells of LEC rats might be activated as effecter cells through STAT-1, T-bet, and NF-κB, resulting in Th1 cytokine production which affect the development of IBD-like lesions of LEC rats.

Treg cells in LEC rats

It has been reported that regulatory immune cells such as $CD4^+CD25^+$ T cells play a crucial role for the pathogenesis of both human IBD and the animal models (21, 22, 24). Thus, we analyzed whether $CD4^+CD25^+$ regulatory T cells influence the development of IBD-like lesions via the immune disorder of LEC rats. First, the cell populations of $CD4^+CD25^+$ T cells in the thymus, spleen, and MLNs form control and LEC rats were analyzed by flow cytometry. $CD4^+CD25^+$ T cells are known to express high levels of Foxp3, a transcription factor that in a normal rat is selectively expressed in $CD25^+$ Treg cells (20). The number of $CD25^+Foxp3^+$ Treg cells of the thymus, spleen, and MLN from LEC rats was significantly lower than that of control rats (Fig. 5, *A* and *B*). In particular, Treg cells of the thymus and MLNs from LEC rats were reduced in contrast to control rats (thymus; $p = 0.0113$, MLN; $p = 0.0133$). Moreover, $Foxp3^+CD4^+$ T cells in MLN from LEC rats were significantly reduced relative to that from control rats (Fig. 5*B*). Interestingly, $Foxp3^+$ Tregs in MLNs (5.12 ± 0.71%) from control rats were markedly increased relative to that in the thymus (0.43 ± 0.11%) and spleen (2.04 ± 0.34%) as shown in Fig. 5*B*. We next assessed the mRNA expression of Foxp3 in the thymus, spleen, and MLNs from LEC and control rats using real-time quantitative RT-PCR. Consistent with the results of flow cytometric analysis (Fig. 5, *A* and *B*), mRNA expression of Foxp3 in the thymus and MLNs from LEC rats was significantly reduced relative to that from control rats (Fig. 5*C*). The prominent expression of Foxp3 mRNA in MLNs from both LEC and control rats was observed comparing with that of the thymus and spleen from both groups (Fig. 5*C*). Furthermore, we confirmed the protein levels of Foxp3 using the nuclear extracts of $CD4^+$ T cell in the thymus, spleen, and MLNs from LEC and control rats by Western

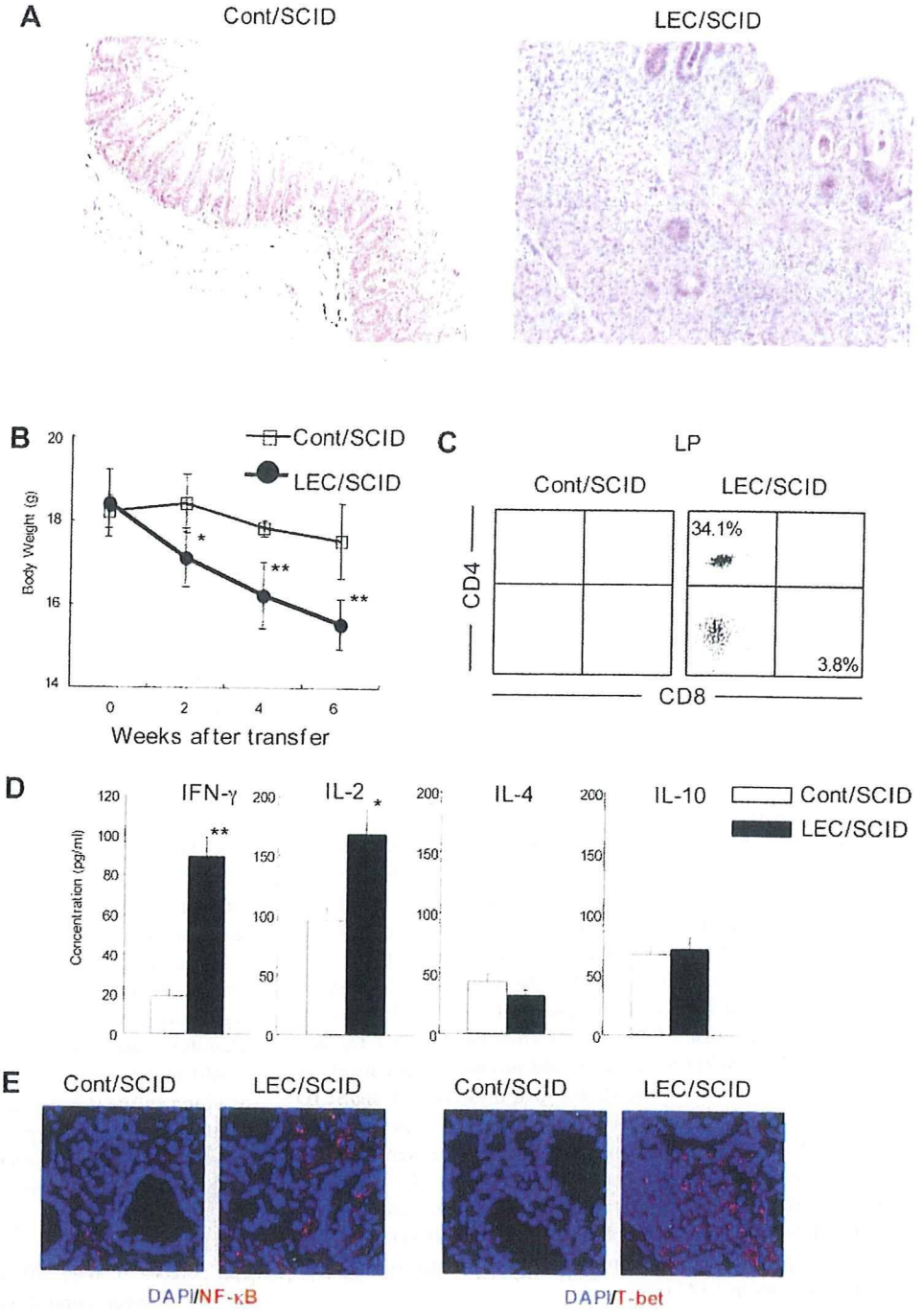

FIGURE 7. Transferable lesions of LEC rats into SCID mice. The pooled MLN T cells (5×10^6) from LEC and control rats were transferred i.p. into SCID mice as recipients. The SCID mice were analyzed at 6 wk after transfer. *A*, Induction of colon lesions in recipient SCID mice. Representative photomicrographs (original magnification, ×100) of H&E-stained paraffin sections of colon from Cont/SCID and LEC/SCID recipients were shown. *B*, The change of body weight of Cont/SCID- and LEC/SCID-recipient mice. After transfer body weight of recipient mice was monitored once in 2 wk. The data are shown as the mean ± SD of approximately four to eight mice. *, $p < 0.05$; **, $p < 0.005$ LEC vs control rats. *C*, Infiltrating T cells in the colon tissues of recipient mice. Purified lymphocytes from the LP in colon of recipient mice were stained with PE-conjugated CD4 mAb and FITC-conjugated CD8 mAb, and analyzed by flow cytometry. Figures were representative of approximately four to eight samples. *D*, Th1-shifted cytokine pattern of LEC/SCID recipients. The supernatants from MLN cells stimulated with CD3-CD28 ligation for 24 h were used to detect the concentration of cytokine productions by ELISA. The data are shown as the mean ± SD of triplicate samples. *, $p < 0.05$; **, $p < 0.005$ LEC/SCID vs Cont/SCID recipients. *E*, NF-κB and T-bet expressions of LPMCs colon were detected by staining with the first mAbs, Alexa 568-conjugated anti-mouse IgG as the second Ab, and DAPI. Photos are representative of three samples.

blotting. As expected, the protein expression of Foxp3 in the thymus and MLNs from LEC rats was markedly lower, and its expression in the spleen from LEC was slightly decreased, compared with the control rats (Fig. 5*D*). Moreover, to clarify the function of Treg cells from LEC rats, T cell suppression assay was performed. Namely, $CD25^-CD4^+$ T cells from control rats were stimulated with plate-coated anti-CD3 mAb and cocultured with control or LEC Treg cells. Although control Treg cells suppressed T cell response considerably, the suppressive function of LEC Treg cells was significantly impaired (Fig. 5*E*). In addition, when $Foxp3^+$ Treg cells in the each segment of colon including cecum, proximal, and distal colon were analyzed, $Foxp3^+$ cells of LPMCs from all segments in LEC rats were significantly decreased compared with those in control rats (Fig. 5*F*). These findings suggest that the decreased $CD4^+CD25^+Foxp3^+$ Tregs in the thymus, MLNs, and LPMCs might affect the intestinal immunity associated with IBD-like lesions in LEC rats.

Treg cells from bone marrow (BM) cells of LEC rats

To know whether the decreased number of Treg cells in LEC rats is derived from the BM cells or not, the BM cells from LEA or LEC rats were transferred into irradiated LEA rats. The number of $Foxp3^+CD25^+CD4^+$ Treg cells in thymus, spleen, and MLNs of chimeric rats was analyzed by flow cytometry. In parallel with the decreased numbers of Treg cells from LEC rats, the $Foxp3^+$ Treg cells of thymus, spleen, and MLNs in the chimeric rats transferred with LEC BM cells were significantly reduced compared with those from LEA BM cells (Fig. 6*A*). Moreover, as to the expansion of T cells from BM cells, although thymocytes and spleen cells of LEC BM cell transplantation (BMT) rats were slightly decreased

Table I. *Induction of IBD-like lesions of LEC rats into SCID mice*

Transfer[a]	Incidence %[b]	Induction/Total
SCID control	0	0/5
Cont/spleen→SCID	0	0/4
LEC/spleen→SCID	0	0/4
Cont/MLN→SCID	0	0/7
LEC/MLN→SCID	87.5	7/8

[a] Purified T cells of MLN or spleen from LEC and control rats were transferred into SCID mice. Six weeks later, histological analysis of colon lesions from SCID recipients was performed.
[b] Incidence of IBD-like lesions was evaluated using four to eight SCID recipients.

compared with those of LEA BMT rats, a significantly increased cell number of MLN from LEC BMT rats was observed (Fig. 6*B*). These findings indicate that the precursor of Treg may exist in the BM, and that the generation of Treg precursors in LEC rats might be deficient in the BM in addition to the deficiency of thymic differentiation.

Induction of IBD-like lesions by adoptive transfer of MLN T cells from LEC rats into SCID mice

To determine whether inflammatory bowel lesions of LEC rats could be induced in SCID mice via a T cell-mediated pathway, adoptive transfer of T cells in MLNs from LEC rats into SCID mice was performed. Importantly, inflammatory lesions of transferred SCID mice with MLN T cells were observed restrictedly in the colon, while no lesion was detected in Cont/SCID recipients at this stage (Fig. 7*A* and Table I). In addition to the IBD-like lesions, the body weight of LEC/SCID recipients transferred with MLN T cells from LEC rats was significantly decreased after the transfer compared with that from Cont/SCID recipients (Fig. 7*B*), whereas there was no change for Cont/SCID recipients. By contrast, adoptive transfer of splenic T cells from LEC rats did not induce any lesions in the SCID recipient (Table I). A large number of $CD4^+$ T cell population was observed within the infiltrating T cells from IBD-like lesions in IBD/SCID recipients (Fig. 7*C*). Moreover, it was demonstrated that MLN T cells stimulated with CD3 and CD28 from LEC/SCID recipients could produce higher levels of IL-2 and IFN-γ, not IL-4 and IL-10, than those from Cont/SCID recipients (Fig. 7*D*). Furthermore, the increased expressions of NF-κB and T-bet in LPMCs from LEC/SCID mice were detected compared with those from Cont/SCID mice (Fig. 7*E*). These results indicate that the IBD-like lesions of LEC rats can be transferred with MLN T cells, not splenic T cells, into SCID mice, and that Th1 response may play a pivotal role in the pathogenesis of IBD-like lesions in LEC rats.

Discussion

As for the animal models of IBD, there have been two categories reported previously (1). One is a spontaneous IBD model with any immune dysfunction such as in IL-$2^{-/-}$, IL-$2R^{-/-}$, IL-$10^{-/-}$, and $NOD2^{-/-}$ mice (18, 41–43). The other is a model manipulated by any drug, bacteria, and cell transfer (44–48). In this study, we demonstrated that the LEC rat is one of spontaneous IBD models, by which the mechanism is due to the decline of Treg cells and the Th1 shift of the cytokine.

T lymphocytes play a central role for the intestinal immune system (12, 49). Recent studies suggested that the balance between Th1 and Th2 cytokines secreted by T cells appears to regulate IBD (13, 39, 48). In this study, the pattern of cytokine production of MLN cells and LPMCs, but not spleen cells, in LEC rats had clearly shifted to Th1. It was reported that the proliferative response of peripheral T cells in LEC rats against T cell mitogen such as Con A had decreased, and that IL-2 production of T cells in LEC rats had reduced (32). However, we found here that proliferative response and Th1 cytokine production of MLN T cells through the TCR/CD3 and CD28 pathway had increased compared with that of control rats. The response of MLN T cells or LPMCs which may regulate the intestinal immune system seems to be different from that of spleen cells from a point of view of cytokine production, and any other immune functions. Namely, MLNs and LPMCs have unique functions regulating the intestinal immune system with exposure to numerous food, bacterial, and/or endogenous Ags. It is possible that defective thymic selection for differentiation into CD4SP cells form DP cells in LEC rats might influence any function including cytokine production in the peripheral T cells. It is well known that cytokine production of immune cells can be occurred through various stimuli such as microorganisms, inflammations, and mechanical or physiological stresses (45, 50–52). The balance between Th1 and Th2 cytokine production is controlled by a number of transcriptional factors and signaling molecules (4). Recent studies indicated that GATA-3 and T-bet might play a central role in controlling the balance of cytokine production from Th cells (4–7). We demonstrated here that Th1 response in MLN T cells and LPMCs through T-bet, STAT-1, and NF-κB might be considerably enhanced, and then the T cell response to numerous intestinal Ags could be responsible for the development of IBD-like lesions in LEC rats.

$CD4^+CD25^+Foxp3^+$ Treg cells have been widely investigated to be generated from the thymus and regulate the peripheral T cells (20). The defective thymic selection of LEC rat influences positive selection into $CD4^+$ from $CD4^+CD8^+$ cells, and results in the dysfunction of peripheral $CD4^+$ T cells (32). It has been reported that Treg cells can prevent IBD-like lesions induced by naive $CD4^+$ T cell transfer into T cell-deficient mice, and regulate Th1 effectors producing IFN-γ (24). In this study, it is speculated that the dysfunction of Treg cells in LEC rats might be associated with the hyperactivation of Th1 effectors in the periphery. In particular, Treg cells in MLNs and LPMCs might play a crucial role for regulating the immune response against numerous intestinal Ags. Therefore, the dysfunction of Treg cells in MLNs and LPMCs would be associated with the deficiency of intestinal tolerance, resulting in the development of IBD-like lesions in LEC rats. In contrast, although $Foxp3^+CD25^-$T cells were reported to have suppressive functions similar to those of $Foxp3^+CD25^+$ classical Treg cells in normal mice (53), there was no difference in the $Foxp3^+CD25^-$T cells (percent) of thymus (control; 0.063 ± 0.011%, LEC; 0.068 ± 0.018%), spleen (control; 0.25 ± 0.04%, LEC; 0.20 ± 0.06%), MLNs (control; 0.47 ± 0.07%, LEC; 0.41 ± 0.06%) between control and LEC rats. The $Foxp3^+CD25^+$ Treg cells, but not $Foxp3^+CD25^-$T cells, of LEC rats might influence the development of colitis of LEC rats.

Direct in vivo evidence of T cell-dependent IBD-like lesions of LEC rats is the induction of the lesion into SCID mice by adoptive transfer with MLN T cells from LEC rats. Although defective T cell functions have been previously reported using fetal thymus grafts of LEC rats into SCID mice, the inflammatory lesions in general have not been investigated (54). Although it is not unclear whether the precursor of Treg cell is generated in BM, the experiment using BM chimera of LEC and LEA rats may imply the origin of the Treg precursor in BM cells.

The LEC rat has been also reported to be used as an animal model for Wilson's disease and developed hepatitis from four months after birth because of the genetic copper metabolism disorder. At a later age, chronic hepatitis and hepatocellular carcinoma are observed in LEC rats (36, 55). The LEC rats have been useful in studying mechanisms of spontaneous carcinogenesis.

Generally described, it has been shown that the pathogenesis of colon cancer could be associated with chronic inflammation such as IBD (56). Previous studies demonstrated that there was a high frequency of 7 *N*-methyl-*N*-nitrosourea-induced colon adenocarcinoma in LEC rats was observed compared with that of control rats (57). It can be speculated that IBD-like inflammatory lesions of LEC rats might affect the carcinogenesis via any indirect mechanism. Although LEC rats were described to have the defective differentiation of CD4 SP cells in the thymus, the decline of peripheral $CD4^+$ T cells, and the failure of proliferative response to T cell mitogen in $CD4^+$ T cells, any inflammatory disease based on these immune disorders has not been investigated. In contrast, the mutation of Th immunodeficiency (*thid*) gene was previously reported (58), which might be associated with immune disorder of LEC rats. Our study focused on Treg cells and cytokine switching as the mechanisms of IBD-like lesions of LEC rats. It is still unclear whether *thid* gene regulates the generation of Treg cells and cytokine switching through T-bet and STAT-1 leading to NF-κB in $CD4^+$ T cells from LEC rats.

In summary, we demonstrated for the first time that IBD-like lesions developed spontaneously in LEC rats. The dysfunction of Treg cells in the periphery and Th1 shift of cytokine production might play a crucial role for pathogenesis of IBD-like lesions in LEC rats. Analyzing the molecular mechanism for IBD-like lesions in LEC rats will be useful for understanding human IBD based on immune disorder in central and peripheral tolerance.

Acknowledgments

We thank Ai Nagaoka and Satoko Yoshida for their technical assistance.

Disclosures

The authors have no financial conflict of interest.

References

1. Blumberg, R. S., L. J. Saubermann, and W. Strober. 1999. Animal models of mucosal inflammation and their relation to human inflammatory bowel disease. *Curr. Opin. Immunol.* 11: 648–656.
2. Fiocchi, C. 1998. Inflammatory bowel disease: etiology and pathogenesis. *Gastroenterology* 115: 182–205.
3. Fiocchi, C. 2005. Inflammatory bowel disease pathogenesis: therapeutic implications. *Chin. J. Dig. Dis.* 6: 6–9.
4. Rengarajan, J., S. J. Szabo, and L. H. Glimcher. 2000. Transcriptional regulation of Th1/Th2 polarization. *Immunol. Today* 21: 479–483.
5. Zheng, W., and R. A. Flavell. 1997. The transcription factor GATA-3 is necessary and sufficient for Th2 cytokine gene expression in CD4 T cells. *Cell* 89: 587–596.
6. Asnagli, H., and K. M. Murphy. 2001. Stability and commitment in T helper cell development. *Curr. Opin. Immunol.* 13: 242–247.
7. Neurath, M. F., B. Weigmann, S. Finotto, J. Glickman, E. Nieuwenhuis, H. Iijima, A. Mizoguchi, E. Mizoguchi, J. Mudter, P. R. Galle, et al. 2002. The transcription factor T-bet regulates mucosal T cell activation in experimental colitis and Crohn's disease. *J. Exp. Med.* 195: 1129–1143.
8. Strober, W., I. J. Fuss, and R. S. Blumberg. 2002. The immunology of mucosal models of inflammation. *Annu. Rev. Immunol.* 20: 495–549.
9. Neurath, M. F., S. Finotto, I. J. Fuss, M. Boirivant, P. R. Galle, and W. Strober. 2001. Regulation of T-cell apoptosis in inflammatory bowel disease: to die or not to die, that is the mucosal question. *Trends Immunol.* 22: 21–26.
10. Atreya, R., J. Mudter, S. Finotto, J. Mullberg, T. Jostock, S. Wirtz, M. Schutz, B. Bartsch, M. Holtmann, C. Becker, et al. 2000. Blockade of interleukin 6 trans signaling suppresses T-cell resistance against apoptosis in chronic intestinal inflammation: evidence in Crohn disease and experimental colitis in vivo. *Nat. Med.* 6: 583–588.
11. Plevy, S. E., C. J. Landers, J. Prehn, N. M. Carramanzana, R. L. Deem, D. Shealy, and S. R. Targan. 1997. A role for TNF-α and mucosal T helper-1 cytokines in the pathogenesis of Crohn's disease. *J. Immunol.* 159: 6276–6282.
12. Iijima, H., M. F. Neurath, T. Nagaishi, J. N. Glickman, E. E. Nieuwenhuis, A. Nakajima, D. Chen, I. J. Fuss, N. Utku, D. N. Lewicki, et al. 2004. Specific regulation of T helper cell 1-mediated murine colitis by CEACAM1. *J. Exp. Med.* 199: 471–482.
13. Fuss, I. J., M. Neurath, M. Boirivant, J. S. Klein, C. de la Motte, S. A. Strong, C. Fiocchi, and W. Strober. 1996. Disparate $CD4^+$ lamina propria (LP) lymphokine secretion profiles in inflammatory bowel disease: Crohn's disease LP cells manifest increased secretion of IFN-γ, whereas ulcerative colitis LP cells manifest increased secretion of IL-5. *J. Immunol.* 157: 1261–1270.
14. Neurath, M. F., I. J. Fuss, B. L. Kelsall, D. H. Presky, W. Waegell, and W. Strober. 1996. Experimental granulomatous colitis in mice is abrogated by induction of TGF-β-mediated oral tolerance. *J. Exp. Med.* 183: 2605–2616.
15. Kitani, A., I. J. Fuss, K. Nakamura, O. M. Schwartz, T. Usui, and W. Strober. 2000. Treatment of experimental (Trinitrobensene sulfonic acid) colitis by intranasal administration of transforming growth factor (TGF)-β1 plasmid: TGF-β1-mediated suppression of T helper cell type 1 response occurs by interleukin (IL)-10 induction and IL-12 receptor β2 chain downregulation. *J. Exp. Med.* 195: 41–52.
16. Eckmann, L., and M. Karin. 2005. NOD2 and Crohn's disease: loss or gain of function? *Immunity* 22: 661–667.
17. Girardin, S. E., J. P. Hugot, and P. J. Sansonetti. 2003. Lessons from Nod2 studies: towards a link between Crohn's disease and bacterial sensing. *Trends Immunol.* 24: 652–658.
18. Murray, P. J. 2005. NOD proteins: an intracellular pathogen-recognition system or signal transduction modifiers? *Curr. Opin. Immunol.* 17: 352–358.
19. Watanabe, T., A. Kitani, P. J. Murray, and W. Strober. 2004. NOD2 is a negative regulator of Toll-like receptor 2-mediated T helper type 1 responses. *Nat. Immunol.* 5: 800–808.
20. Sakaguchi, S. 2005. Naturally arising Foxp3-expressing $CD25^+CD4^+$ regulatory T cells in immunological tolerance to self and non-self. *Nat. Immunol.* 6: 345–352.
21. Maul, J., C. Loddenkemper, P. Mundt, E. Berg, T. Giese, A. Stallmach, M. Zeitz, and R. Duchmann. 2005. Peripheral and intestinal regulatory $CD4^+$ $CD25^{high}$ T cells in inflammatory bowel disease. *Gastroenterology* 128: 1868–1878.
22. Fantini, M. C., C. Becker, I. Tubbe, A. Nikolaev, H. A. Lehr, P. R. Galle, and M. F. Neurath. 2005. TGF-β induced $Foxp3^+$ regulatory T cells suppress Th1-mediated experimental colitis. *Gut* 55: 671–680.
23. Singh, B., S. Read, C. Asseman, V. Malmstrom, C. Mottet, L. A. Stephens, R. Stepankova, H. Tlaskalova, and F. Powrie. 2001. Control of intestinal inflammation by regulatory T cells. *Immunol. Rev.* 182: 190–200.
24. Martin, B., A. Banz, B. Bienvenu, C. Cordier, N. Dautigny, C. Becourt, and B. Lucas. 2004. Suppression of $CD4^+$ T lymphocyte effector functions by $CD4^+CD25^+$ cells in vivo. *J. Immunol.* 172: 3391–3398.
25. Niederau, C., F. Backmerhoff, B. Schumacher, and C. Niederau. 1997. Inflammatory mediators and acute phase proteins in patients with Crohn's disease and ulcerative colitis. *Hepatogastroenterology* 44: 90–107.
26. Nielsen, O. H., T. Ciardelli, Z. Wu, E. Langholz, and I. Kirman. 1995. Circulating soluble interleukin-2 receptor α and β chain in inflammatory bowel disease. *Am. J. Gastroenterol.* 90: 1301–1306.
27. Poussier, P., T. Ning, J. Chen, D. Banerjee, and M. Julius. 2000. Intestinal inflammation observed in IL-2R/IL-2 mutant mice is associated with impaired intestinal T lymphopoiesis. *Gastroenterology* 118: 880–891.
28. Sohn, K. J., S. A. Shah, S. Reid, M. Choi, J. Carrier, M. Comiskey, C. Terhorst, and Y. I. Kim. 2001. Molecular genetics of ulcerative colitis-associated colon cancer in the interleukin 2- and β_2-microglobulin-deficient mouse. *Cancer Res.* 61: 6912–6917.
29. El Yousfi, M., M. D. Breuille, I. Papet, S. Blum, M. Andre, L. Mosoni, P. Denis, C. Buffiere, and C. Obled. 2003. Increased tissue protein synthesis during spontaneous inflammatory bowel disease in HLA-B27 rats. *Clin. Sci. Lond.* 105: 437–446.
30. Elson, C. O., Y. Cong, V. J. McCracken, R. A. Dimmitt, R. G. Lorenz, and C. T. Weaver. 2005. Experimental models of inflammatory bowel disease reveal innate, adaptive, and regulatory mechanisms of host dialogue with the microbiota. *Immunol. Rev.* 206: 260–276.
31. Davidson, N. J., M. W. Leach, M. M. Fort, L. Thompson-Snipes, R. Kuhn, W. Muller, D. J. Berg, and D. M. Rennick. 1996. T helper cell 1-type $CD4^+$ T cells, but not B cells, mediate colitis in interleukin 10-deficient mice. *J. Exp. Med.* 184: 241–251.
32. Agui, T., M. Oka, Y. Yamada, T. Sakai, K. Izumi, Y. Ishida, K. Himeno, and K. Matsumoto. 1990. Maturational arrest from $CD4^+8^+$ to $CD4^+8^-$ thymocytes in a mutant strain (LEC) of rat. *J. Exp. Med.* 172: 1615–1624.
33. Sakai, T., T. Agui, K. Wei, M. Oka, H. Hisaeda, H. Nagasawa, K. Himeno, and K. Matsumoto. 1998. Unresponsiveness of $CD4^-8^{+/-}$ thymocytes to lectin stimulation in LEC mutant rats. *Immunology* 95: 219–225.
34. Collison, L. W., C. J. Workman, T. T. Kuo, K. Boyd, Y. Wang, K. M. Vignali, R. Cross, D. Sehy, R. S. Blumberg, and D. A. A. Vignali. 2007. The inhibitory cytokine IL-35 contributes to regulatory T-cell function. *Nature* 22: 566–571.
35. Xystrakis, E., A. S. Dejean, I. Bernard, P. Druet, R. Liblau, D. Gonzalez-Dunia, and A. Saoudi. 2004. Identification of a novel natural regulatory CD8 T-cell subset and analysis of its mechanism of regulation. *Blood* 104: 3294–3301.
36. Li, Y., Y. Togashi, S. Sato, T. Emoto, J. H. Kang, N. Takeichi, H. Kobayashi, Y. Kojima, Y. Une, and J. Uchida. 1991. Spontaneous hepatic copper accumulation in Long-Evans Cinnamon rats with hereditary hepatitis: a model of Wilson's disease. *J. Clin. Invest.* 87: 1858–1861.
37. Yamazaki, K., H. Ohyama, K. Kurata, and T. Wakabayashi. 1993. Effects of dietary vitamin E on clinical course and plasma glutamic oxaloacetic transaminase and glutamic pyruvic transaminase activities in hereditary hepatitis of LEC rats. *Lab. Anim. Sci.* 43: 61–67.
38. Das, J., C. H. Chen, L. Yang, L. Cohn, P. Ray, and A. Ray. 2001. A critical role for NF-κB in GATA3 expression and TH2 differentiation in allergic airway inflammation. *Nat. Immunol.* 2: 45–50.
39. Hwang, E. S., J. H. Hong, and L. H. Glimcher. 2005. IL-2 production in developing Th1 cells is regulated by heterodimerization of RelA and T-bet and requires T-bet serine residue 508. *J. Exp. Med.* 202: 1289–1300.
40. Torgerson, T. R., A. D. Colosia, J. P. Donahue, Y. Z. Lin, and J. Hawiger. 1998. Regulation of NF-κB, AP-1, NFAT, and STAT1 nuclear import in T lymphocytes

by noninvasive delivery of peptide carrying the nuclear localization sequence of NF-κB p50. *J. Immunol.* 161: 6084–6092.
41. Sadlack, B., H. Merz, H. Schorle, A. Schimpl, A. C. Feller, and I. Horak. 1993. Ulcerative colitis-like disease in mice with a disrupted interleukin-2 gene. *Cell* 75: 253–261.
42. Asseman, C., S. Mauze, M. W. Leach, R. L. Coffman, and F. Powrie. 1999. An essential role for interleukin 10 in the function of regulatory T cells that inhibit intestinal inflammation. *J. Exp. Med.* 190: 995–1004.
43. Eckmann, L. 2004. Innate immunity and mucosal bacterial interactions in the intestine. *Curr. Opin. Gastroenterol.* 20: 82–88.
44. Brimnes, J., J. Reimann, M. Nissen, and M. Claesson. 2001. Enteric bacterial antigens activate CD4 $^+$ T cells from *scid* mice with inflammatory bowel disease. *Eur. J. Immunol.* 31: 23–31.
45. Kullberg, M. C., J. F. Andersen, P. L. Gorelick, P. Caspar, S. Suerbaum, J. G. Fox, A. W. Cheever, D. Jankovic, and A. Sher. 2003. Induction of colitis by a CD4$^+$ T cell clone specific for a bacterial epitope. *Proc. Natl. Acad. Sci. USA* 100: 15830–15835.
46. Aranda, R., B. C. Sydora, P. L. McAllister, S. W. Binder, H. Y. Yang, S. R. Targan, and M. Kronenberg. 1997. Analysis of intestinal lymphocytes in mouse colitis mediated by transfer of CD4$^+$, CD45RB^{high} T cells to SCID recipients. *J. Immunol.* 158: 3464–3473.
47. Powrie, F., M. W. Leach, S. Mauze, S. Menon, L. B. Caddle, and R. L. Coffman. 1994. Inhibition of Th1 responses prevents inflammatory bowel disease in *scid* mice reconstituted with CD45RB^{hi} CD4$^+$ T cells. *Immunity* 1: 553–562.
48. Kanai, T., T. Kawamura, T. Dohi, S. Makita, Y. Nemoto, T. Totsuka, and M. Watanabe. 2006. TH1/TH2-mediated colitis induced by adoptive transfer of CD4$^+$CD45RB^{high} T lymphocytes into nude mice. *Inflamm. Bowel. Dis.* 12: 89–99.
49. Breese, E., C. P. Braegger, C. J. Corrigan, J. A. Walker-Smith, and T. T. MacDonald. 1993. Interleukin-2- and interferon-γ-secreting T cells in normal and diseased human intestinal mucosa. *Immunology* 78: 127–131.
50. Lodes, M. J., Y. Cong, C. O. Elson, R. Mohamath, C. J. Landers, S. R. Targan, M. Fort, and R. M. Hershberg. 2004. Bacterial flagellin is a dominant antigen in Crohn disease. *J. Clin. Invest.* 113: 1296–1306.
51. Fiorucci, S., E. Antonelli, E. Distrutti, P. Del Soldato, R. J. Flower, M. J. Clark, A. Morelli, M. Perretti, and L. J. Ignarro. 2002. NCX-1015, a nitric-oxide derivative of prednisolone, enhances regulatory T cells in the lamina propria and protects against 2,4,6-trinitrobenzene sulfonic acid-induced colitis in mice. *Proc. Natl. Acad. Sci. USA* 99: 15770–15775.
52. Zhou, P., R. Borojevic, C. Streutker, D. Snider, H. Liang, and K. Croitoru. 2004. Expression of dual TCR on DO11.10 T cells allows for ovalbumin-induced oral tolerance to prevent T cell-mediated colitis directed against unrelated enteric bacterial antigens. *J. Immunol.* 172: 1515–1523.
53. Zelenay, S., T. L. Carvalho, I. Caramalho, M. F. M. Fontes, M. Rebelo, and J. Demengeot. 2005. Foxp$^+$CD25$^+$CD4 T cells constitute a reservoir of committed regulatory cells that regain CD25 expression upon homeostatic expansion. *Proc. Natl. Acad. Sci. USA* 102: 4091–4096.
54. Chai, J. G., T. Sakai, H. Hisaeda, H. Nagasawa, K. Yasutomo, A. Furukawa, H. Ishikawa, Y. Maekawa, H. Uehara, K. Izumi, et al. 1996. Development of functional rat-derived T cells in SCID mice engrafted with the fetal thymus of LEC rats which are defective in CD4$^+$ T cells. *Microbiol. Immunol.* 40: 659–664.
55. Choudhury, S., R. Zhang, K. Frenkel, T. Kawamori, F. L. Chung, and R. Roy. 2003. Evidence of alterations in base excision repair of oxidative DNA damage during spontaneous hepatocarcinogenesis in Long Evans Cinnamon rats. *Cancer Res.* 63: 7704–7707.
56. Itzkowitz, S. 2003. Colon carcinogenesis in inflammatory bowel disease: applying molecular genetics to clinical practice. *J. Clin. Gastroenterol.* 36: S70–S74; discussion S94-76.
57. Min, H., E. Kudo, A. Hino, K. Yoshimoto, H. Iwahana, M. Itakura, and K. Izumi. 1997. *p53* gene mutation in *N*-butyl-*N*-(4-hydroxybutyl)nitrosamine-induced urinary bladder tumors and *N*-methyl-*N*-nitrosourea-induced colon tumors of rats. *Cancer Lett.* 117: 81–86.
58. Wei, K., Y. Muramatsu, T. Sakai, T. Yamada, and K. Matsumoto. 1997. Chromosomal mapping of the T-helper immunodeficiency (*thid*) locus in LEC rats. *Immunogenetics* 47: 99–102.

Crosstalk between RANKL and Fas signaling in dendritic cells controls immune tolerance

Takashi Izawa,[1,2] Naozumi Ishimaru,[1] Keiji Moriyama,[2] Masayuki Kohashi,[1] Rieko Arakaki,[1] and Yoshio Hayashi[1]

[1]Department of Oral Molecular Pathology, Institute of Health Biosciences, The University of Tokushima Graduate School, Kuramotocho, Tokushima, Japan; [2]Department of Orthodontics and Dentofacial Orthopedics, Institute of Health Biosciences, The University of Tokushima Graduate School, Kuramotocho, Tokushima, Japan

Although receptor activator of nuclear factor (NF)–κB ligand (RANKL) signaling has been shown to prolong the survival of mature dendritic cells (DCs), the association of RANKL pathway with Fas-mediated apoptosis is obscure. Here, we found that bone marrow–derived DCs (BMDCs) from the Fas-deficient strain *MRL/lpr* mice, could survive much longer than normal DCs. The expressions of Bcl-x and Bcl-2 and the nuclear transport of NF-κB of RANKL-stimulated BMDCs from *MRL/lpr* mice were significantly upregulated. By contrast, Fas expression of BMDCs from normal C57BL/6 and *MRL*$^{+/+}$ mice was increased by RANKL stimulation, and an enhanced DC apoptosis was found when stimulated with both RANKL and anti-Fas mAb, which was associated with activation of caspase-3 and caspase-9. Furthermore, the expression of FLIP$_L$, an inhibitory molecule against Fas-mediated apoptosis, in normal DCs was significantly decreased by RANKL and anti-Fas mAb. Indeed, the adoptive transfer of RANKL-stimulated DCs resulted in rapid acceleration of autoimmunity in *MRL/lpr* recipients. These findings indicate that the crosstalk between RANKL and Fas signaling in DCs might control immune tolerance. (Blood. 2007;110:242-250)

Introduction

Dendritic cells (DCs) are professional antigen-presenting cells that reside in peripheral tissues in an immature state for optimal antigen uptake and respond to inflammatory signals.[1,2] After capture of pathogen-derived antigens and activation by pathogens, DCs migrate from tissues to the lymphoid organs where DCs become mature and initiate antigen-specific T cells.[1,2] While many subpopulations of DCs have been reported to be heterogeneous in their phenotype and localized in lymphoid tissues, there is general agreement that DCs originate from a hematopoietic progenitor, and that there are 3 DC subtypes, including myeloid DCs ($CD11c^+CD11b^+CD8\alpha^-$), lymphoid DCs ($CD11c^+CD11b^-CD8\alpha^+$), and plasmacytoid DCs ($CD11c^+B220^+Gr\text{-}1^+$), all of which have been recently identified.[3-6]

The lifespan of activated antigen-bearing DCs has been estimated to be as short as 3 days.[7,8] Limiting the lifespan of DCs by means of apoptosis may serve to regulate the availability of antigen for T cells and to control immune responses. An important and well-characterized mechanism for apoptosis in immune cells is mediated by Fas, the death receptor.[9] Although Fas has been implicated in the apoptosis of DCs,[10,11] DCs are known to be resistant to Fas-induced cell death.[12] In addition, it has been reported that the resistance to Fas-induced apoptosis in DCs correlates with the consititutive expression of the Fas-associated death domain–like IL-1β–converting enzyme (FLICE)–inhibitory protein (FLIP) ligand.[13] However, the molecular mechanism for maintenance of DCs through Fas-mediated signals is still unclear.

Receptor activator of nuclear factor (NF)–κB ligand (RANKL),[14,15] a type II membrane protein of the tumor necrosis factor (TNF) family, is expressed on osteoblasts, stromal cells, and activated T cells,[15] and binds to the signaling receptor RANK and the decoy receptor osteoprotegerin (OPG).[15,16] Mice lacking RANKL or RANK display dramatically reduced osteoclastogenesis, show defects in early differentiation of T and B cells, systemic lymph nodes, and fail to develop mammary glands.[17,18] Moreover, recent data have showed that the interaction of Fas ligand and Fas expressed on osteoclast precursors increases RANKL-induced osteoclastogenesis.[19] On the other hand, RANKL-RANK interaction has been shown to prolong the survival of mature DCs, whereas the association of the RANKL pathway with Fas-mediated signals in the activation or function of DCs has been obscure.[15,20]

In this study, to define the molecular mechanism for the autoimmunity by immune dysregulation of DCs through Fas and the RANKL pathway, the *MRL/lpr* mouse strain, an autoimmune-prone strain that has a mutated Fas gene, was used to analyze the immune functions of the DCs and autoimmunity such as rheumatoid lesions.

Materials and methods

Mice

MRL/Mp-lpr/lpr (*MRL/lpr*; aged 4-12 weeks; n = 105), *MRL*$^{+/+}$ mice (aged 4-12 weeks; n = 55), and C57BL/6 (B6; n = 50) mice were purchased from Charles River Japan Inc. (Atsugi, Japan). All mice were maintained in specific pathogen–free conditions in our animal facility, and the experiments were approved by an animal ethics board of Tokushima University (Tokushima, Japan).

Submitted November 28, 2006; accepted March 8, 2007. Prepublished online as *Blood* First Edition paper, March 19, 2007; DOI 10.1182/blood-2006-11-059980.

The online version of this article contains a data supplement.

The publication costs of this article were defrayed in part by page charge payment. Therefore, and solely to indicate this fact, this article is hereby marked "advertisement" in accordance with 18 USC section 1734.

Generation of murine BMDCs

A crude population of DCs was generated in vitro from mouse bone marrow as described with some modifications.[21,22] Briefly, bone marrow was flushed from the long bones of the limbs. Cells were plated at a density of 1×10^6 and were cultured for 7 days in 5% CO_2 at 37°C in RPMI 1640 medium containing 10% heat-inactivated fetal bovine serum (FBS), 100 U/mL penicillin, 10 ng/mL recombinant mouse granulocyte-monocyte colony-stimulating factor (GM-CSF; PeproTech, Le Perray-en-Yvelines, France), and 5 ng/mL mouse IL-4 (PeproTech). DCs ($CD11c^+$ cells, < 70%) including mainly immature DCs (50% $CD11c^+CD86^-$ cells, < 50%) were routinely used for the experiments.

Flow cytometric analysis

Bone marrow–derived DCs (BMDCs) were stained with fluorescein isothiocyanate (FITC)–conjugated anti-CD11c mAb, along with rat anti–major histocompatibility complex class II (MHC class II; $I\text{-}A^k$) as primary Ab and phycoerythin (PE)–conjugated anti-rat IgG as secondary Ab. BMDCs were also stained with PE–anti-CD86, PE–anti-CD80, or anti–Bcl-2, anti–Bcl-xL, and PE–anti-rat IgG. For each staining, isotype-matched mAb was used as a control. All mAbs were obtained from BD Biosciences (San Diego, CA). The cells were analyzed with an EPICS flow cytometer (Beckman Coulter Inc, Miami, FL), and data were analyzed with FlowJo FACS analysis software (Tree Star Inc, Ashland, OR).

Detection of apoptotic cells

Cells were treated with or without 100 ng/mL Fas-activating antibody (Jo-2; BD Biosciences) for 24 to 72 hours and were detected with an EPICS flow cytometer using an Annexin V–FITC apoptosis detection kit (Genzyme, Cambridge, MA). Briefly, after cultured cells were washed in phosphate-buffered saline (PBS), the cells were incubated with FITC-conjugated Annexin-V and propidium iodide (PI) for 10 minutes at room temperature in the dark. Binding buffer was added, and apoptotic cells were detected by flow cytometric analysis with an EPICS flow cytometer.

Measurement of cytokine production

Cytokine production was tested by a 2-step sandwich enzyme-linked immunosorbent assay (ELISA) using a mouse IL-12p40, IL-10, and interferon (IFN)-γ, IL-2, and IL-4 kit (Genzyme, Cambridge, MA). In brief, the culture supernatants from DCs or T cells were added to microtiter plates precoated with anti-IL-12p40, IL-10, IFN-γ, IL-2, and IL-4 capture Ab and incubated overnight at 4°C. After adding biotinylated detecting Ab and incubating at room temperature for 45 minutes, streptavidin-peroxidase was added and incubated again at room temperature for an additional 30 minutes. Finally, an 2,2′-azino-di-3-ethylbenzthiazoline sulfonate substrate containing H_2O_2 was added, and the colorimetric reaction was read at an absorbance of 450 nm using an automatic microplate reader (Bio-Rad Laboratories Inc, Hercules, CA). The concentration was calculated according to the standard curves produced by various concentrations of recombinant cytokines.

MTT assay

The effect of RANKL on proliferation of BMDCs was determined by the MTT dye uptake method. Briefly, the cells (2000/well) were incubated in triplicate in a 96-well plate in the presence or absence of RANKL in a final volume of 0.1 mL for the indicated time periods at 37°C. Then, 0.025 mL MTT solution (5 μg/mL in PBS) was added to each well. After incubation at 37°C for 2 hours, 0.1 mL of the extraction buffer (20% sodium dodecyl sulfide [SDS], 50% dimethylformamide) was added. Incubation was continued overnight at 37°C, and then the optical density (OD) was measured at 450 nm using an automatic microplate reader (Flow, McLean, VA), with the extraction buffer as blank.

Western blot analysis

The cell extracts from the nucleus and cytoplasm of DCs were prepared using the Nuclear/Cytosol Fractionation Kit (Bio Vision, Mountain View, CA). Cells were briefly washed, collected in ice-cold PBS in the presence of phosphatase inhibitors, and centrifuged at 230*g* for 5 minutes. The pellets were resuspended in a hypotonic buffer, treated with detergent, and centrifuged at 14 000*g* for 30 seconds. After collection of the cytoplasmic fraction, the nuclei were lysed and nuclear proteins were solubilized in lysis buffer containing protease inhibitors. A total of 50 μg of each sample per well was used for SDS–polyacrylamide gel electrophoresis. After blocking with 5% nonfat milk, the membrane was incubated with primary antibodies for TRAF6, IKK, p-IκBa, NF-κB p65 (RelA), and p50 (Santa Cruz Biotechnology, Santa Cruz, CA). Antibody-antigen complexes were detected using a horseradish peroxidase–conjugated secondary antibody. Protein binding was visualized with enhanced chemiluminescence Western blotting reagent (Amersham Biosciences, Arlington Heights, IL). Western blotting using anti–Bcl-2, anti–Bcl-xL, anti-Bax, anti-Bid (BD Bioscience), anti–caspase-3, anti–caspase-8, and anti–caspase-9 Abs (Cell Signaling Technology, Beverly, MA), and anti-$FLIP_L$ (Santa Cruz Biotechnology) was performed essentially as described for the lysis buffer. Control for protein loading was provided by anti-mouse histone, or GAPDH mAb (Sigma Chemical Co, St Louis, MO).

siRNA of Fas and RANK

For small interfering RNA (siRNA) of Fas and RANK, a siTrio Full Set (B-Bridge International, Sunnyvale, CA) was used for analyzing the function of DCs. Briefly, each cocktail including the 3 RNA oligonucleotides listed here was transfected into cells with a Silencer siRNA Transfection II kit (Ambion, Austin, TX). Sequences of the oligonucleotide sets are as follows: Fas, GGGAAGGAGUACAUGGACATT (sense), UGUCCAUGUACUCCUUCCCTT (antisense), CGAAAGUACCGGAAAAGAATT (sense), UUCUUUUCCGGUACUUUCGTT (antisense), CCAGAAGGACCUUGGAAAATT (sense), UUUUCCAAGGUCCUUCUGGTT (antisense); and RANK, CCAAGGAGGCCCAGGCUUATT (sense), UAAGCCUGGGCCUCCUUGGTT (antisense), GGGAAAGCGCUGACAGCUATT (sense), UAGCUGUCAGCGCUUUCCCTT (antisense), CUGAAAAGCACCUGACAAATT (sense), UUUGUCAGGUGCUUUUCAGTT. Transfected cells were incubated with or without RANKL, and flow cytometric analysis was performed.

Confocal microscopic analysis

Immature DCs were seeded onto glass-bottom culture dishes (MatTek, Ashland, MA) at a density of 500 cells/well and stimulated for 30, 60, or 120 minutes with RANKL. Subsequently, cells were washed and fixed in cold 3% paraformaldehyde (PFA) in PBS for 10 minutes, then permeabilized with 0.2% Triton-X in PBS for 2 minutes. The slides were then washed thoroughly with PBS and incubated with optimal dilutions of the primary Ab in PBS containing 1% bovine serum albumin (BSA)–2.5% FBS in PBS for 1 hour at room temperature. Cells were stained with optimal dilutions of the primary Abs for 1 hour. After 3 washes with 0.0001% Triton-X in PBS, the cells were stained with Alexa Fluor 488 goat anti-rabbit IgG (H + L; Molecular Probes, Eugene, OR) or Texas red–conjugated goat anti-mouse (Molecular Probes) as the second Abs for 30 minutes and washed with PBS. For each fluorochrome label, negative control Abs were added. Finally, the slides were incubated with 4′, 6-diamidino-2-phenylindole (DAPI) for 5 minutes to label the nuclei and mounted in Vectashield (Vector Labs, Burlingame, CA) for analysis by confocal microscopy (LSM5 PASCAL, Carl Zeiss, Gottingen, Germany). A 63 × 1.4 oil DIC objective lens was used. Quick Operation Version 3.2 (Carl Zeiss) for imaging acquisition and Adobe Photoshop CS2 (Adobe Systems, San Jose, CA) for image processing were used.

Transfer of DCs

BMDCs were stimulated in vitro for 48 hours with 100 ng/mL RANKL and 50 μg/mL bovine type II collagen (CII). RANKL-stimulated BMDCs were transferred into the base of the tail by subcutaneous injections in 200 μL PBS at the age of 4 weeks.